Ferrara activity 2010-2011

Contalbrigo Marco
Luciano Pappalardo
INFN Ferrara

RICH studies for CLAS12

Preliminary studies with GEANT3 based simulation

Simulations with stand alone Monte Carlo (from Hall-A):

- GEANT3 toolkit
- Simplified geometry
- Ideal optical surfaces
- Rayleigh scattering treated as additional absorption
- No background accounted for

First conclusions:

Aerogel + visible-light detection mandatory to separate pions and kaons in the 2-8 GeV/c momentum range

Preliminary studies of basic parameters:

- Aerogel refractive index and thickness
- Photon detector pixel size
- Gap dimension

Best configuration:

3cm aerogel, n=1.03, gap=1m

$$\langle n\sigma_{\pi K}\rangle \approx 4 \quad (8\,\mathrm{GeV/c},\quad \mathrm{pad} = 1.0\mathrm{cm}^2)$$

$$\langle n\sigma_{\pi K}\rangle \approx 7 \quad (8\,\mathrm{GeV/c},\quad \mathrm{pad} = 0.3\mathrm{cm}^2)$$

Moving to gemc

General framework: GEMC (Maurizio, JLab) + RICH impl. (Ahmed, Argonne)

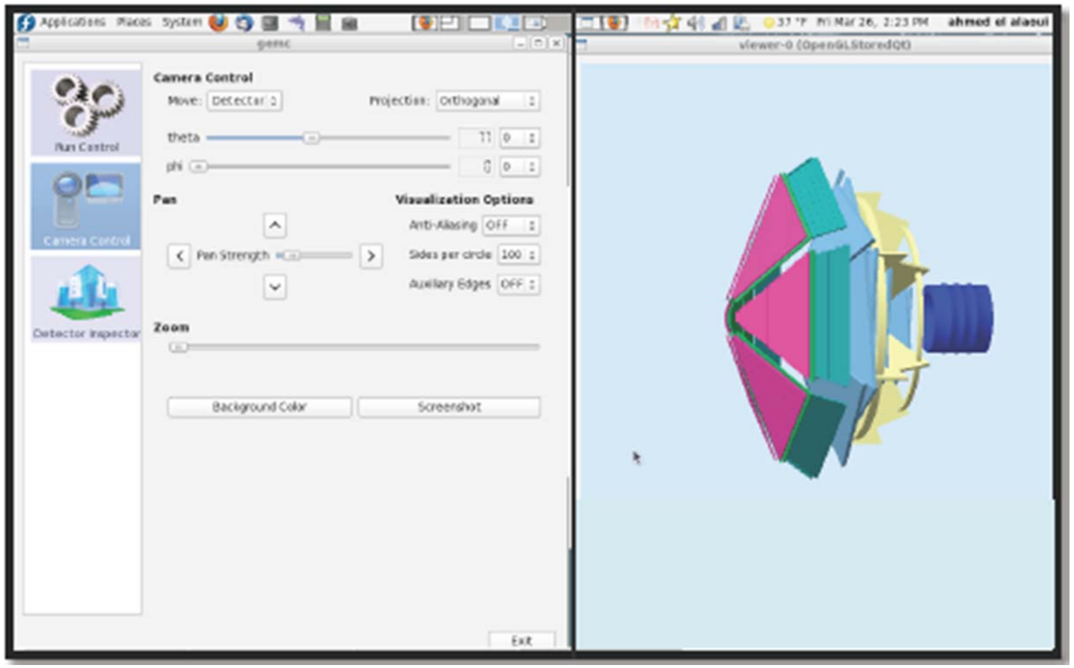

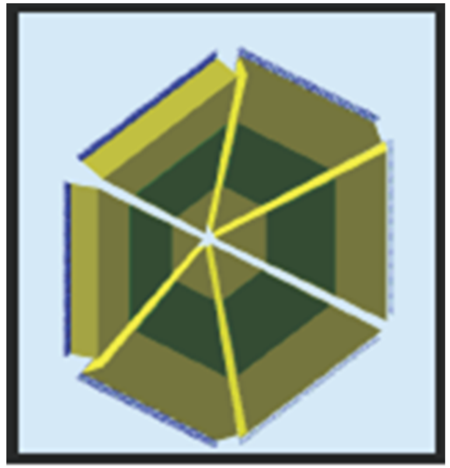

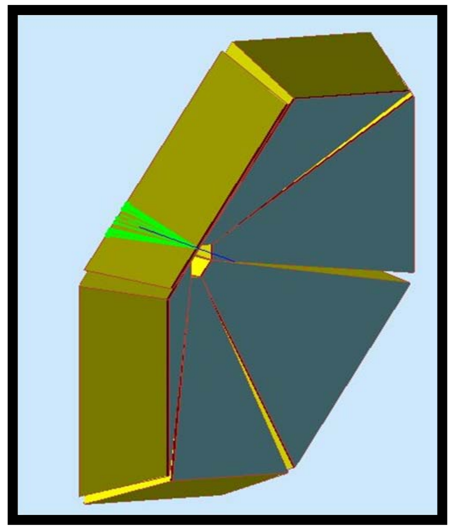

GEANT4 toolkit for a complete simulation:

- realistic geometry / detailed optic effects
- full Cherenkov ring simulation chain
- track multiplicity / background

The focusing mirror system

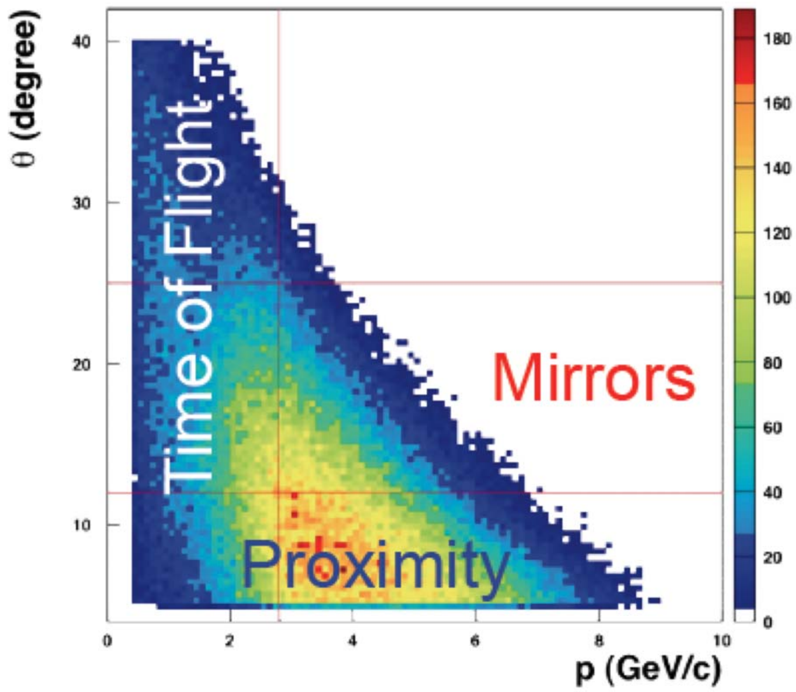

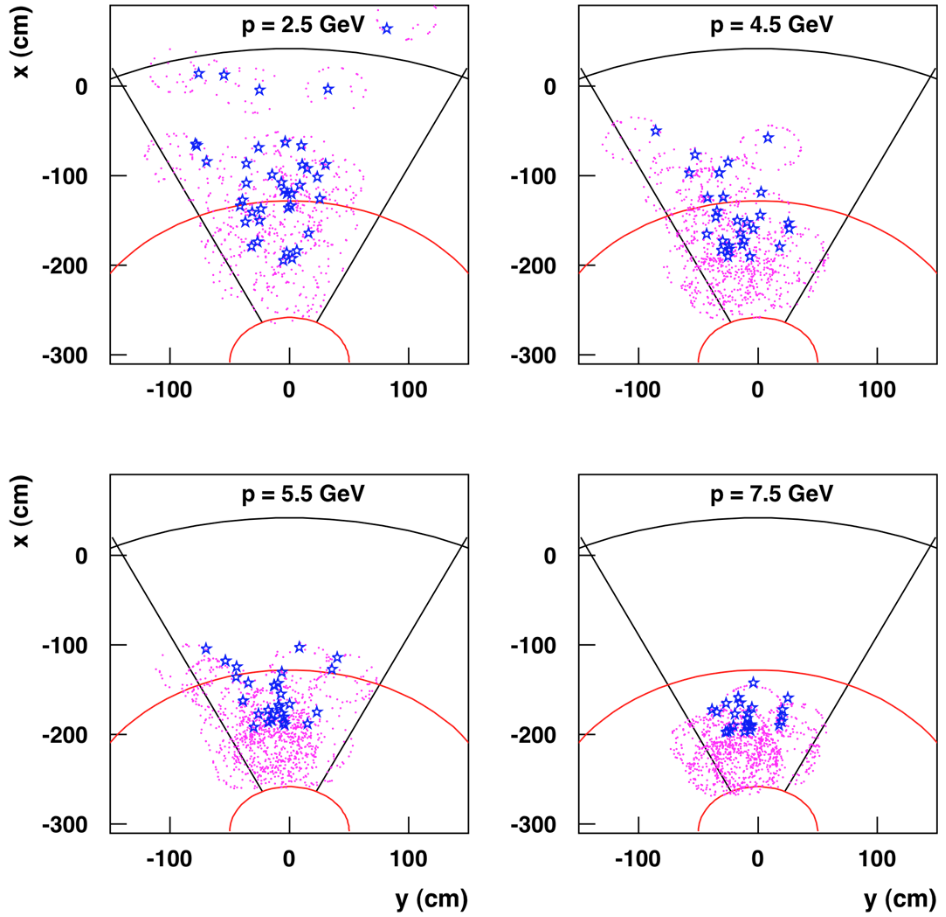

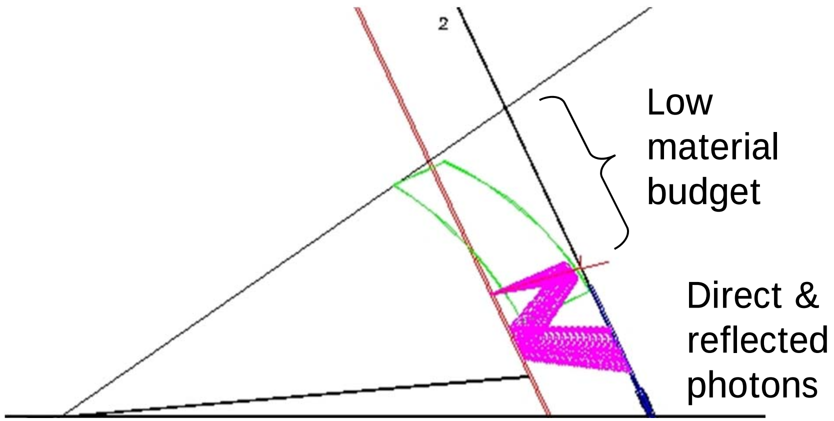

Goals:

- instrument only forward region
- reduce active area (~1 m^2/sect)
- minimize interference with TOF system

The focusing mirror system

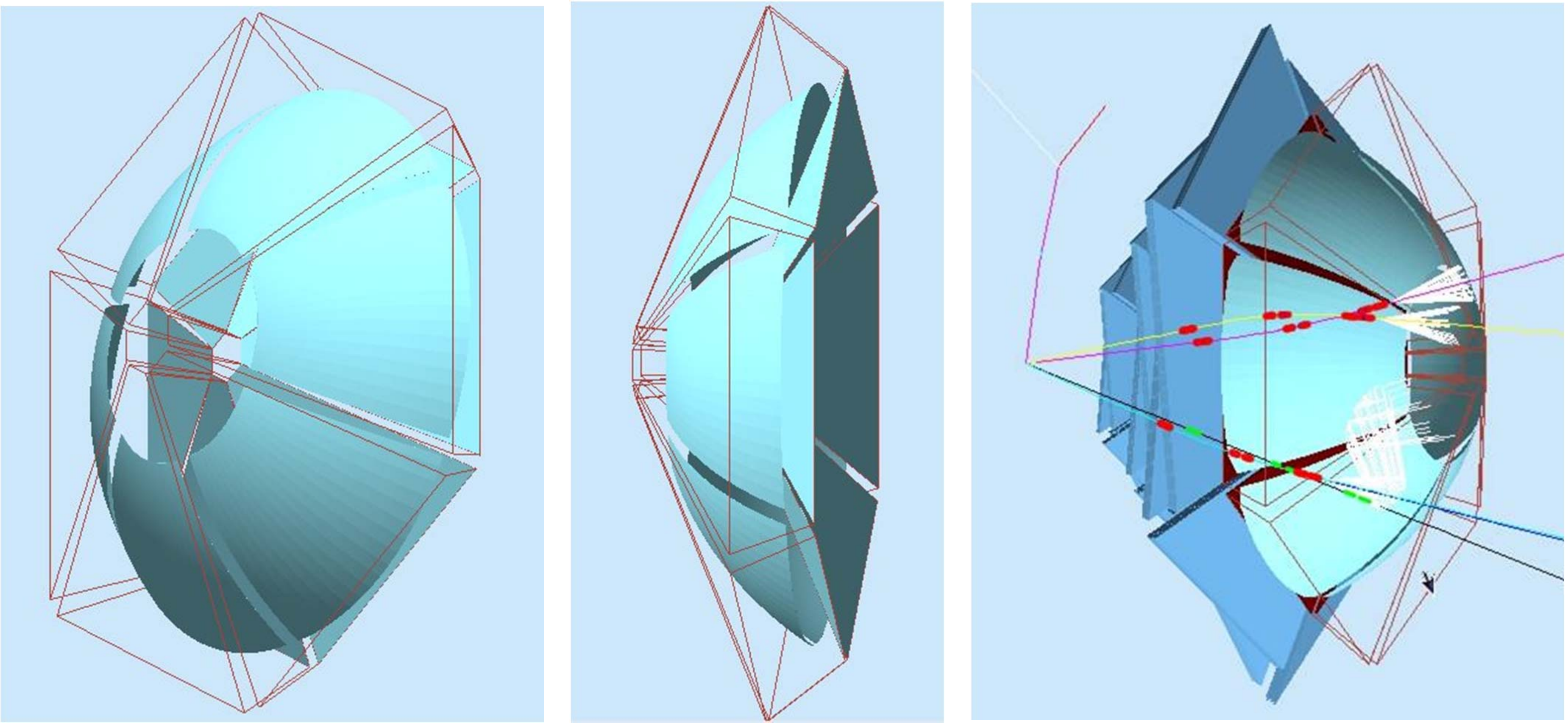

- elliptical mirror within gap volume for backward reflections
- plane mirror just beyond radiator for forward reflections
- combined reflections focalize Cerenkov photons onto photon-detector plane

Testing different aerogel configurations

2 parallel 5 GeV π^+ tracks at θ=15 produced at different x,y coordinates just beyond the radiator (cross same radiator thickness)

"standard scenario": n=1.03, 3cm aerogel, 1m gap

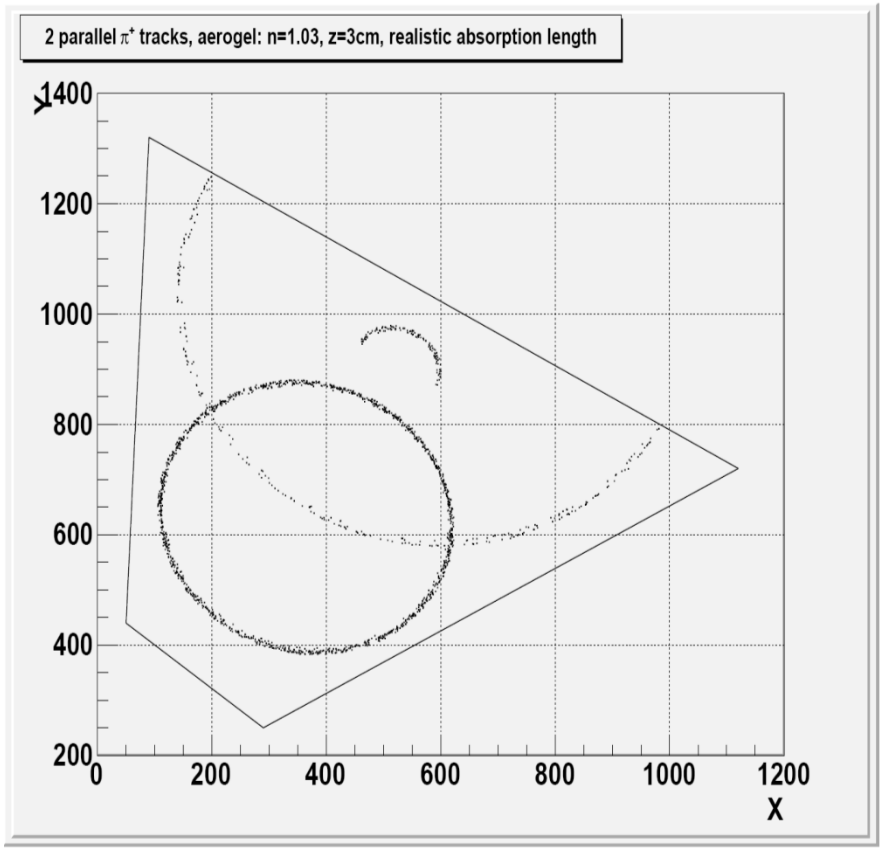

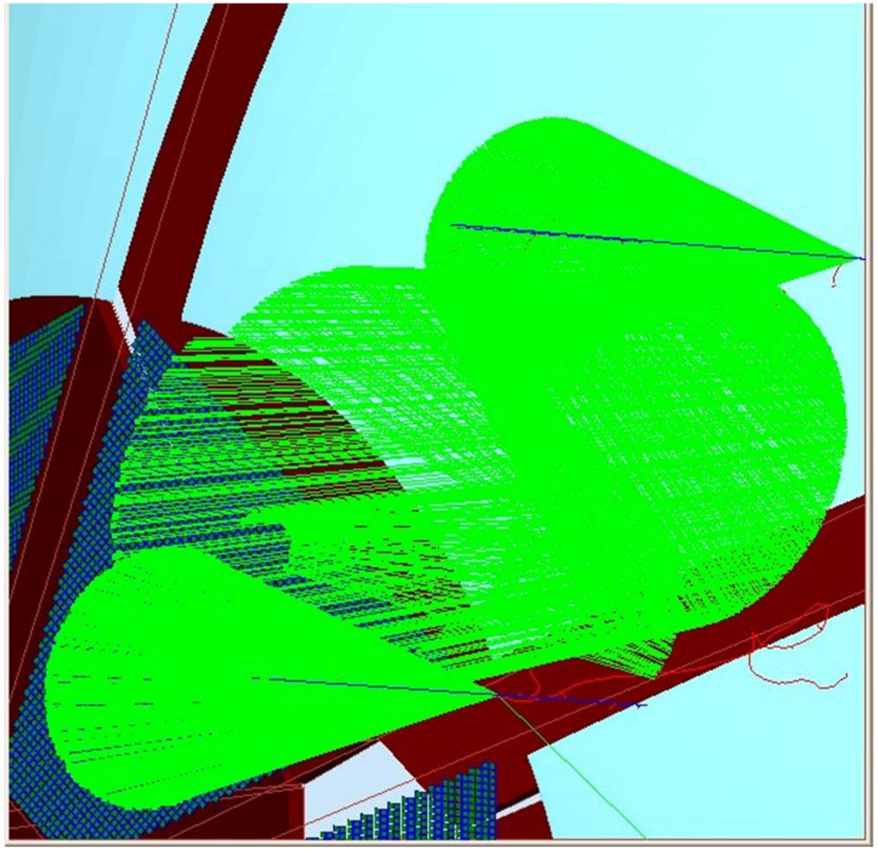

The ring pattern for different particles at 5 GeV/c

π^+ and K^+ rings move towards the "dead region" while π^- and K^- rings appear at low y

"direct" rings for π^- and K^- and "reflected" rings for π^+ and K^+

"reflected rings" for all mesons show two components

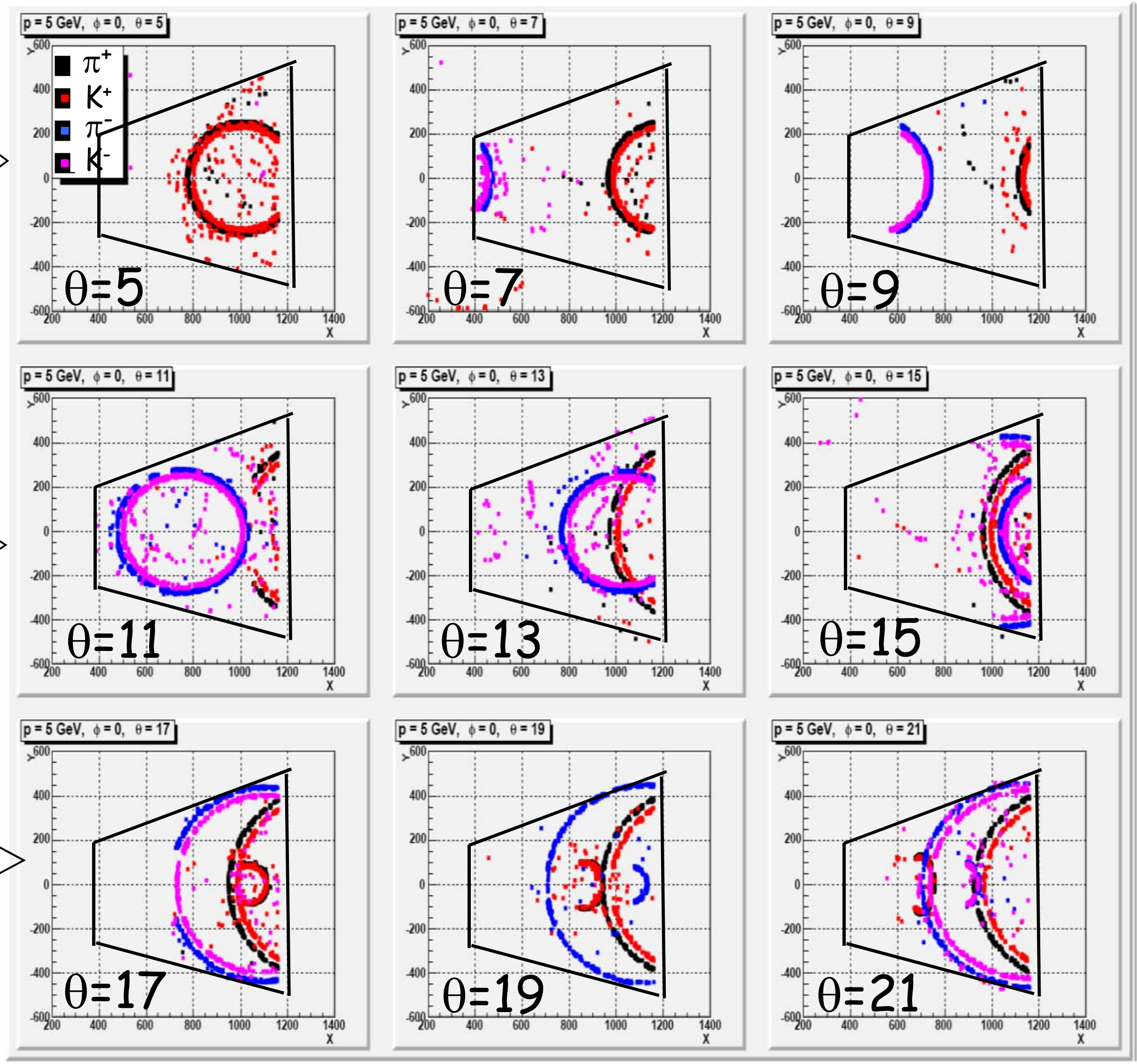

Testing different aerogel configurations

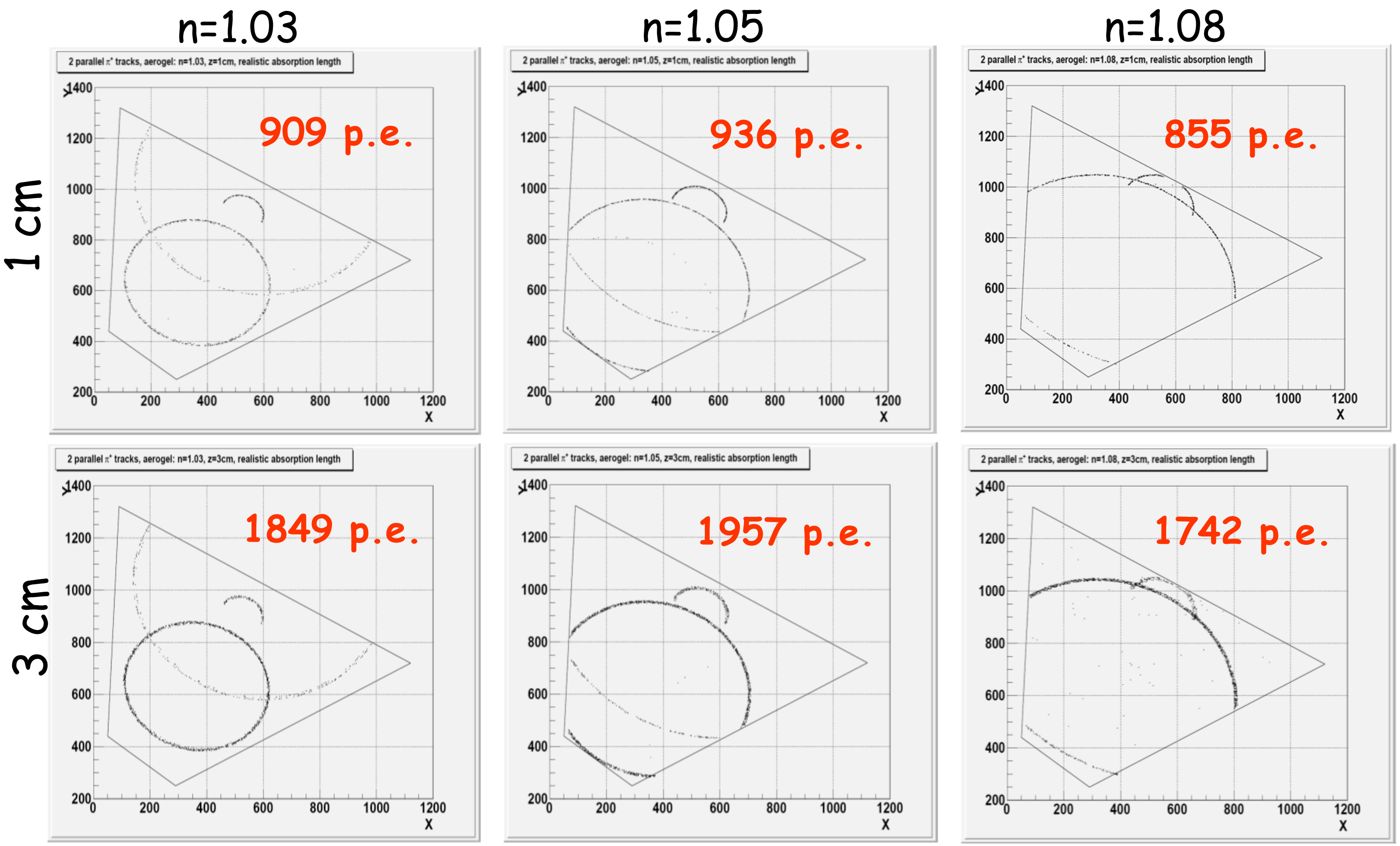

- larger n results in larger rings: for n=1.08 most of the direct ring is lost
- part of lost photons (outside sector) may be recollected using a continuous detector (no sectors)
- larger thickness ensures more photons despite enhanced absorption

Testing different aerogel configurations

DIRECT RINGS				
π tracks	n	thickness	Tot p.e.	Av. p.e.
25	1.03	1 cm	587	3.5
25	1.03	2 cm	958	5.8
25	1.03	3 cm	1459	8.8
25	1.05	1 cm	612	3.8
25	1.05	2 cm	1069	6.4
25	1.05	3 cm	1541	9.1
25	1.08	1 cm	529	3.2
25	1.08	2 cm	944	5.7
25	1.08	3 cm	1428	8.4

REFLECTED RINGS				
π tracks	n	thickness	Tot p.e.	Av. p.e.
25	1.03	1 cm	322	1.8
25	1.03	2 cm	381	2.1
25	1.03	3 cm	390	2.1
25	1.05	1 cm	324	1.8
25	1.05	2 cm	385	2.1
25	1.05	3 cm	416	2.1
25	1.08	1 cm	326	1.8
25	1.08	2 cm	344	1.8
25	1.08	3 cm	314	1.6

DIRECT RINGS:

- average number of p.e. increases with radiator thickness
- n=1.05 provides a bit more p.e. in average

REFLECTED RINGS:

- average number of p.e. insensitive of radiator thickness and n
- not sufficient for ring reconstruction $\Rightarrow$ improve mirror geometry mandatory
- try "multi-layer" radiator option

Progresses done (1)

✓ Optimization of mirror geometry to minimize the "dead region" (reflected photons were not focalized on detector at certain intermediate angles)

✓ Optimization of RICH geometry -> joint sectors

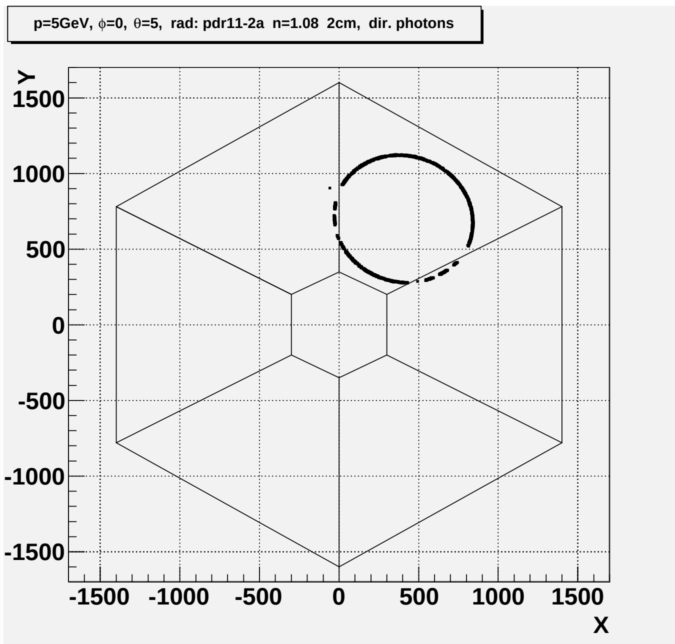

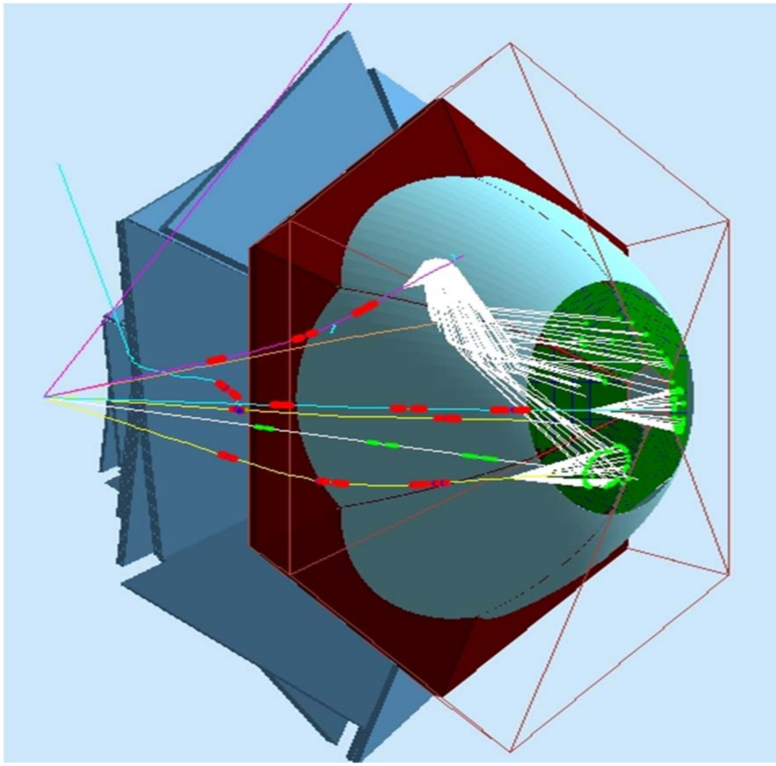

Progresses done (2)

✓ Investigate multi-layer (2 or more) aerogel options: e.g. thicker radiator at larger angles (more photons produced in case of reflection) to compensate for absorption in multiple crossing of radiator material

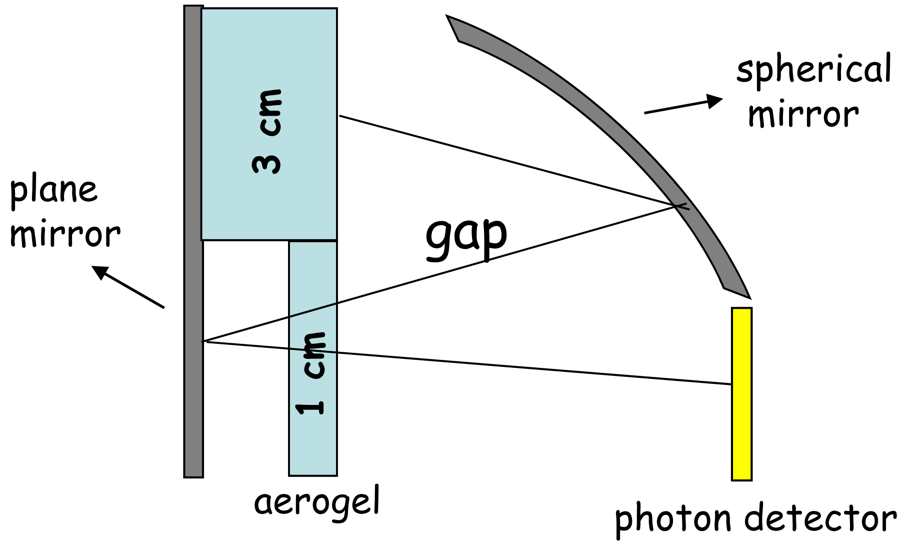

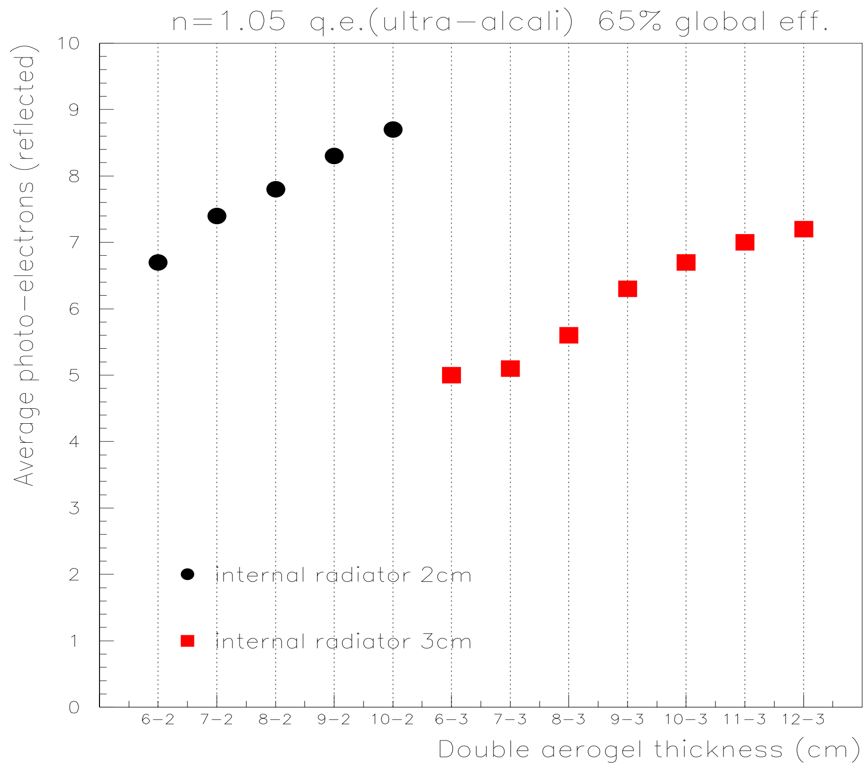

→ Thickness 2-4-6-8-10 cm

Progresses done (3)

✓ Investigate different configurations (semi-reflective mirror in front of aerogel)

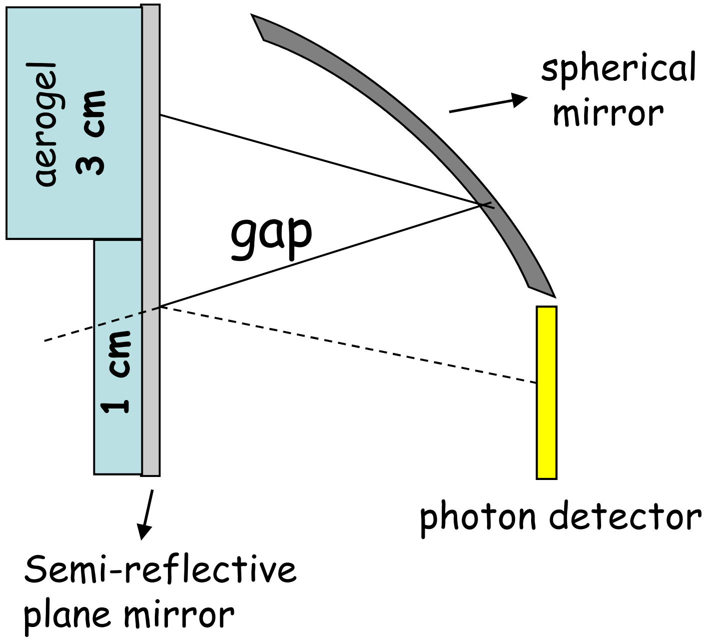

→ …but no real improvements in number of p.e.

➢ **Reconstruction algorithm** (so far only used for systematic studies on number of p.e.)

The reconstruction algorithm

For a given track t and particle hypothesis h $(=\pi, K, p)$ use **direct ray tracing** for a large number of generated photons to determine the **hit probability for each PMT**

The **measured hit pattern** is compared to the hit **probability densities** for the different hypotheses through a likelihood function:

$$L^{(h,t)} = \Sigma_i log[P^{(h,t)}_{PMT}(i) C_{PMT}(i) + \overline{P}^{(h,t)}_{PMT}(i)(1 - C_{PMT}(i))]$$

(the hypothesis that maximizes $\mathbf{L}^{(\mathbf{h},\mathbf{t})}$ is assumed to be true)

$C_{PMT}(i)$ is the hit pattern from data
- = 1 if the ith PMT is hit
- = 0 if the ith PMT is not hit

$P^{(h,t)}_{PMT}(i)$ is the probability of a hit given the kinematics of track t and hypothesis h

$$P^{(h,t)}_{PMT}(i) = 1 - exp(-\frac{N^{(h,t)}(i)}{\Sigma_i N^{(h,t)}(i)} n^{(h,t)} - B(i))$$

$\overline{P}^{(h,t)}_{PMT}(i) = 1 - P^{(h,t)}_{(PMT)}$ is the probability of no hit

$n^{(h,t)}$ is the total number of expected PMT hits

$B(i)$ is a background term

The reconstruction algorithm

Mirror: 14-25º

PMTs: UBA

200 trials per point

Aerogel:

- n=1.06
- thick. increasing with radius: 2-4-6-8-10 cm

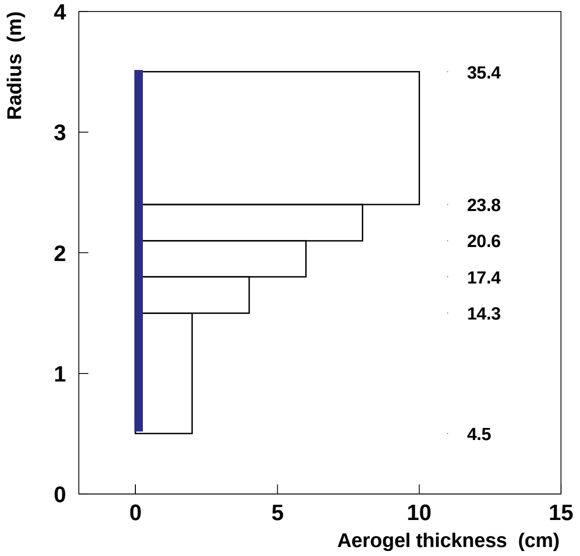

The reconstruction algorithm

Mirror: 14-25°

PMTs: UBA

200 trials per point

Aerogel:
- n=1.06
- thick. increasing with radius: 2-4-6-8-10 cm

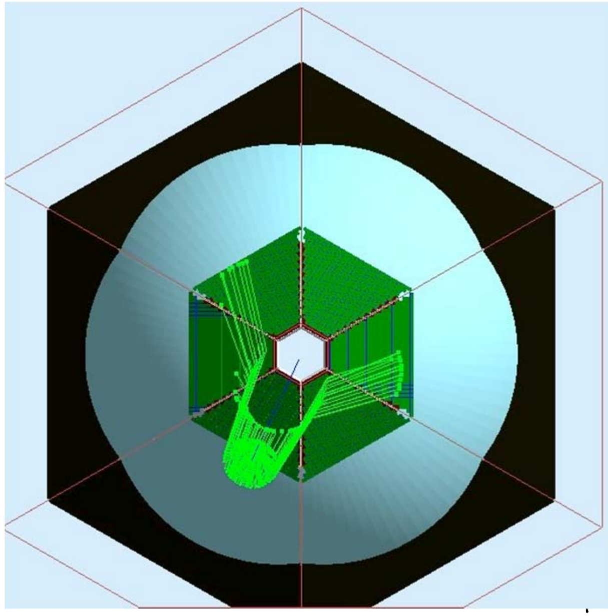

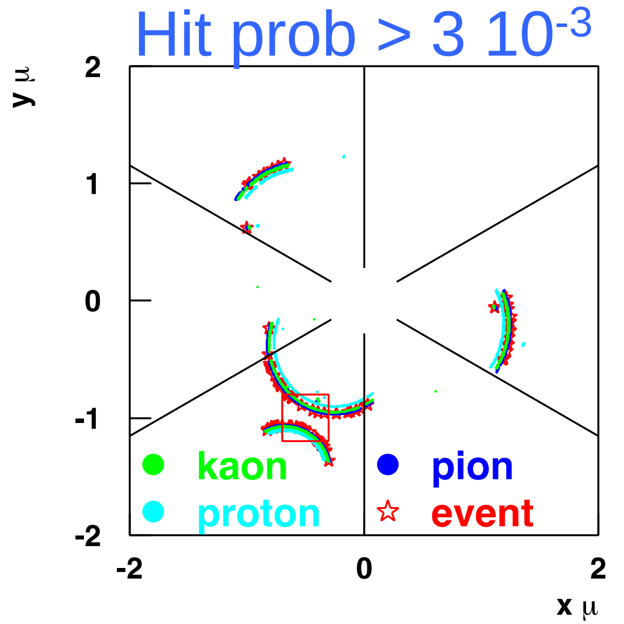

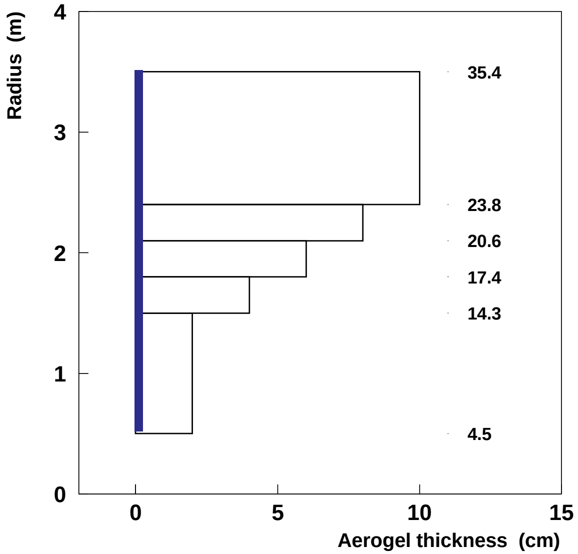

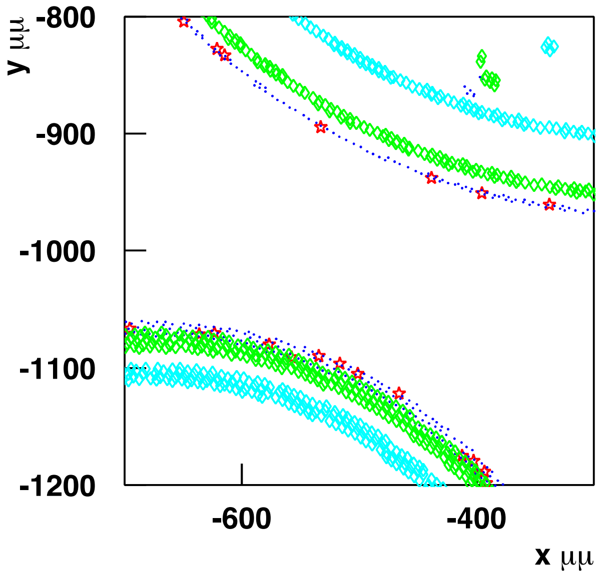

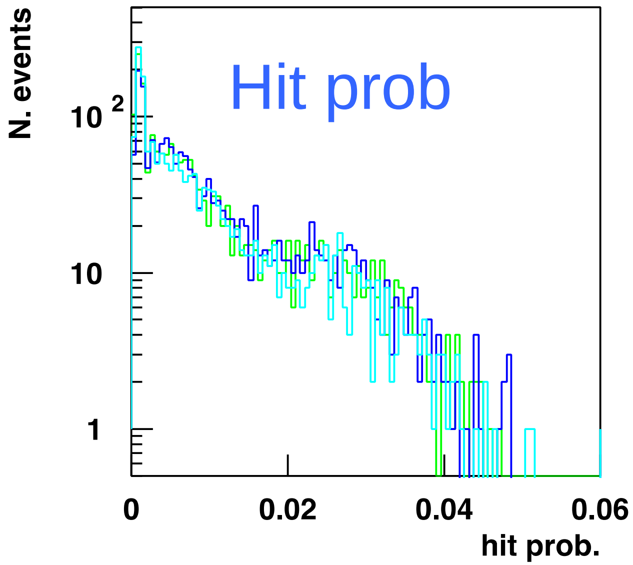

LH_{π}-$LH_{k,p}$: Mirror 14-25° PMTs: UBA

200 trials per point

Aerogel:

- n=1.06
- thick. increasing with radius: 2-4-6-8-10 cm

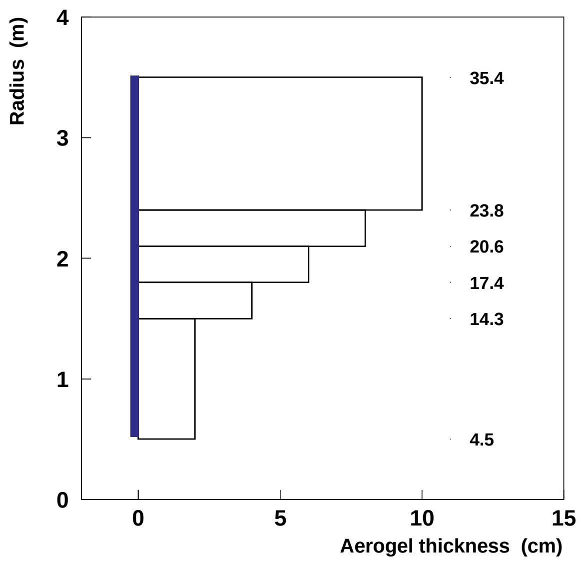

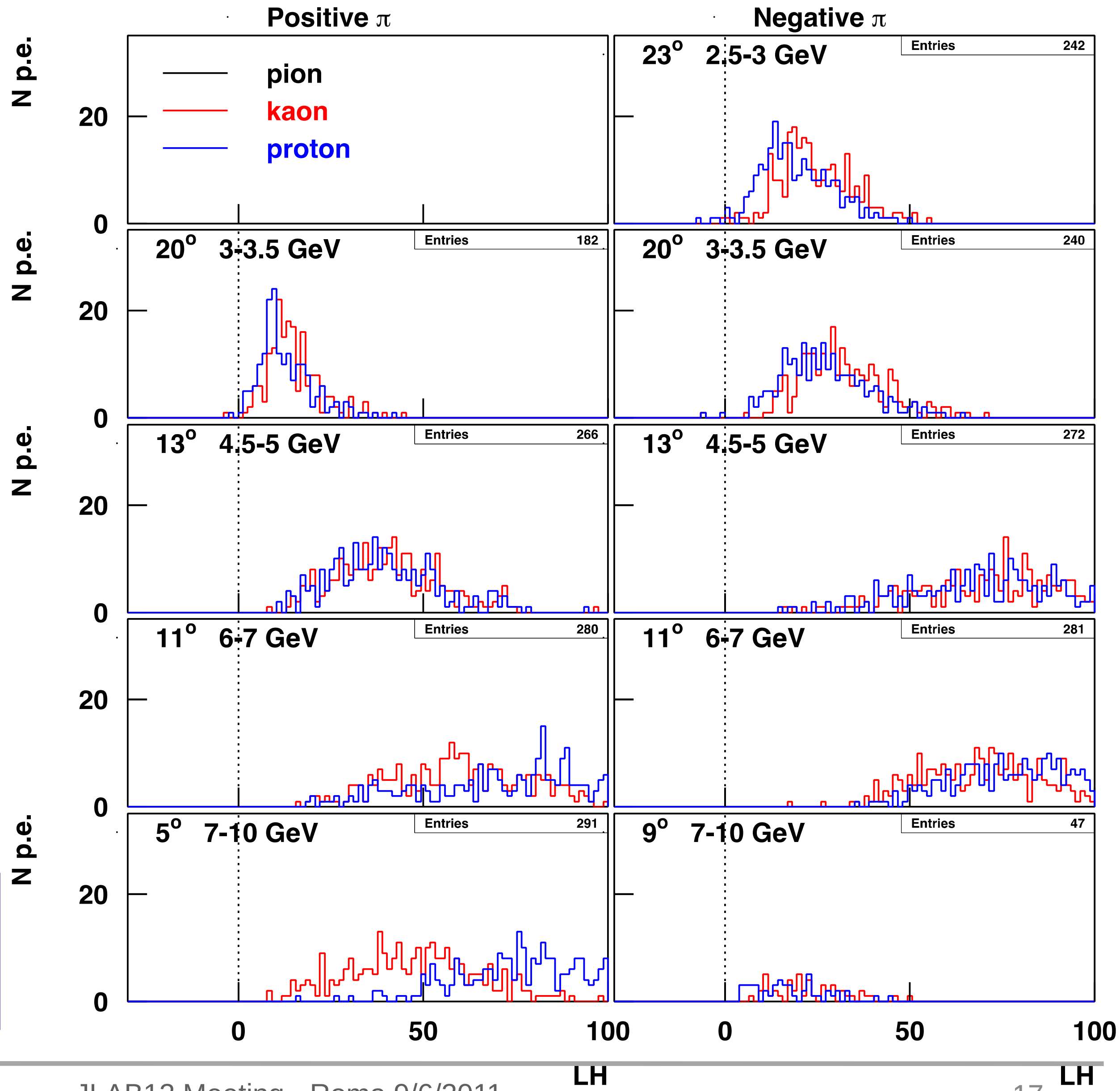

Low angles more challenging
The same with increased number of trials

Average N p.e. : Mirror 14-25º   PMTs: UBA

200 trials per point

Aerogel:

- n=1.06
- thick. increasing with radius: 2-4-6-8-10 cm

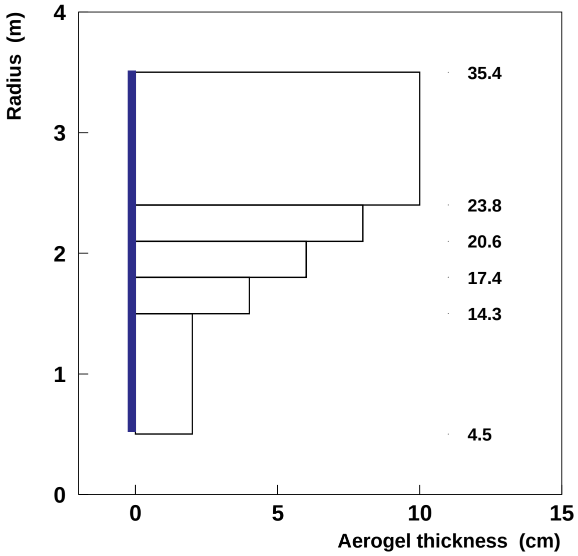

N p.e. > 5 for reflected rings
N p.e. > 12 for direct rings

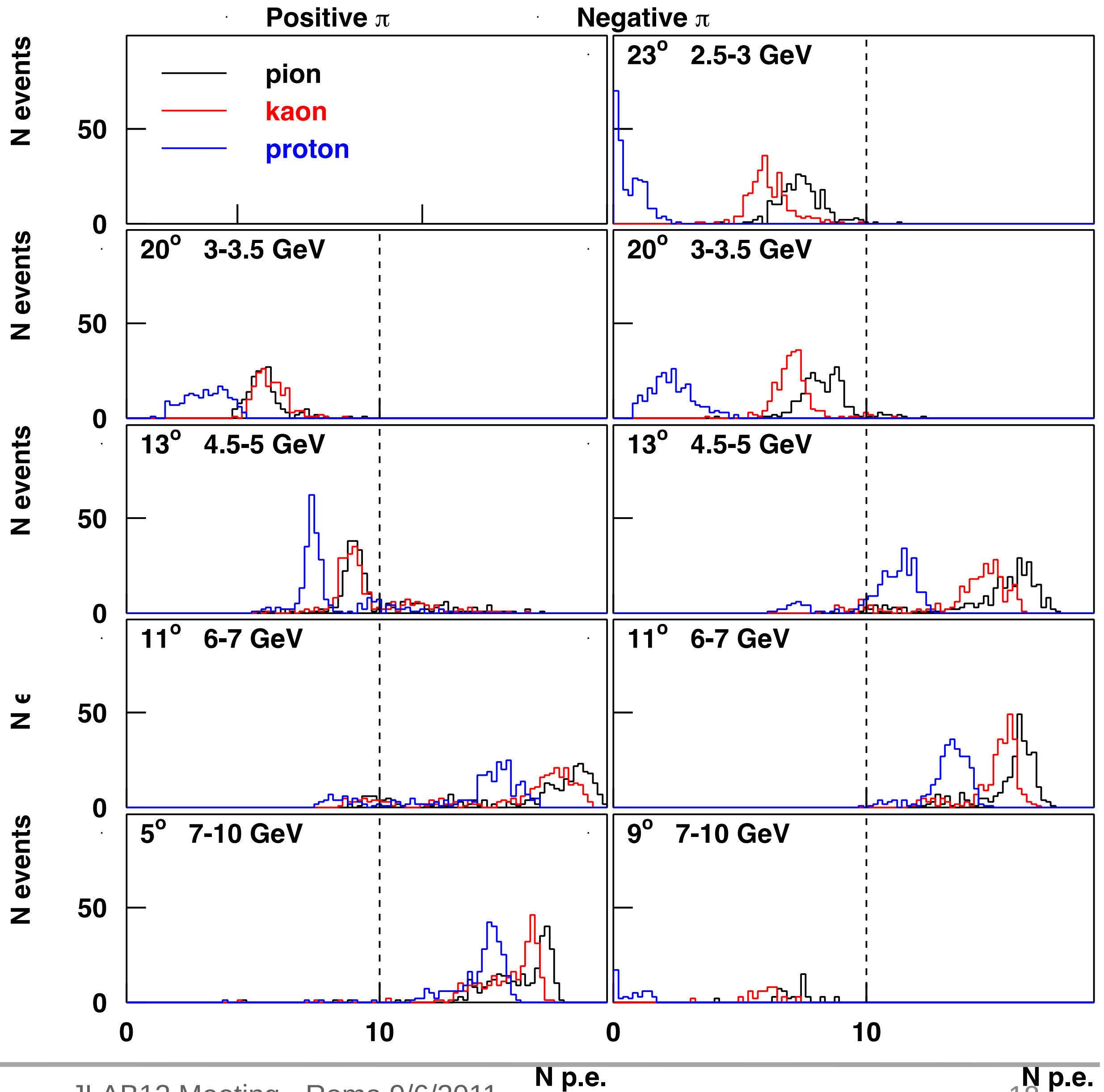

Average N p.e. : Mirror 14-25^o PMTs: UBA

200 trials per point

Aerogel:

- n=1.06
- thick. increasing with radius: 2-4-6-8-10 cm

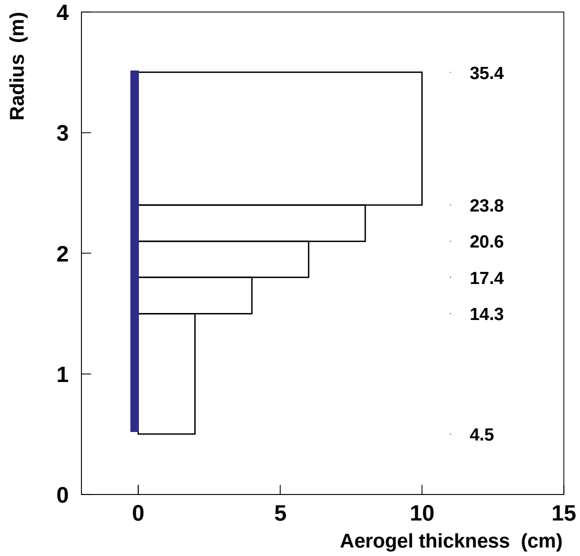

Mirror is mandatory for positive hadrons and gives benefit for negative hadrons at large angles and small energy

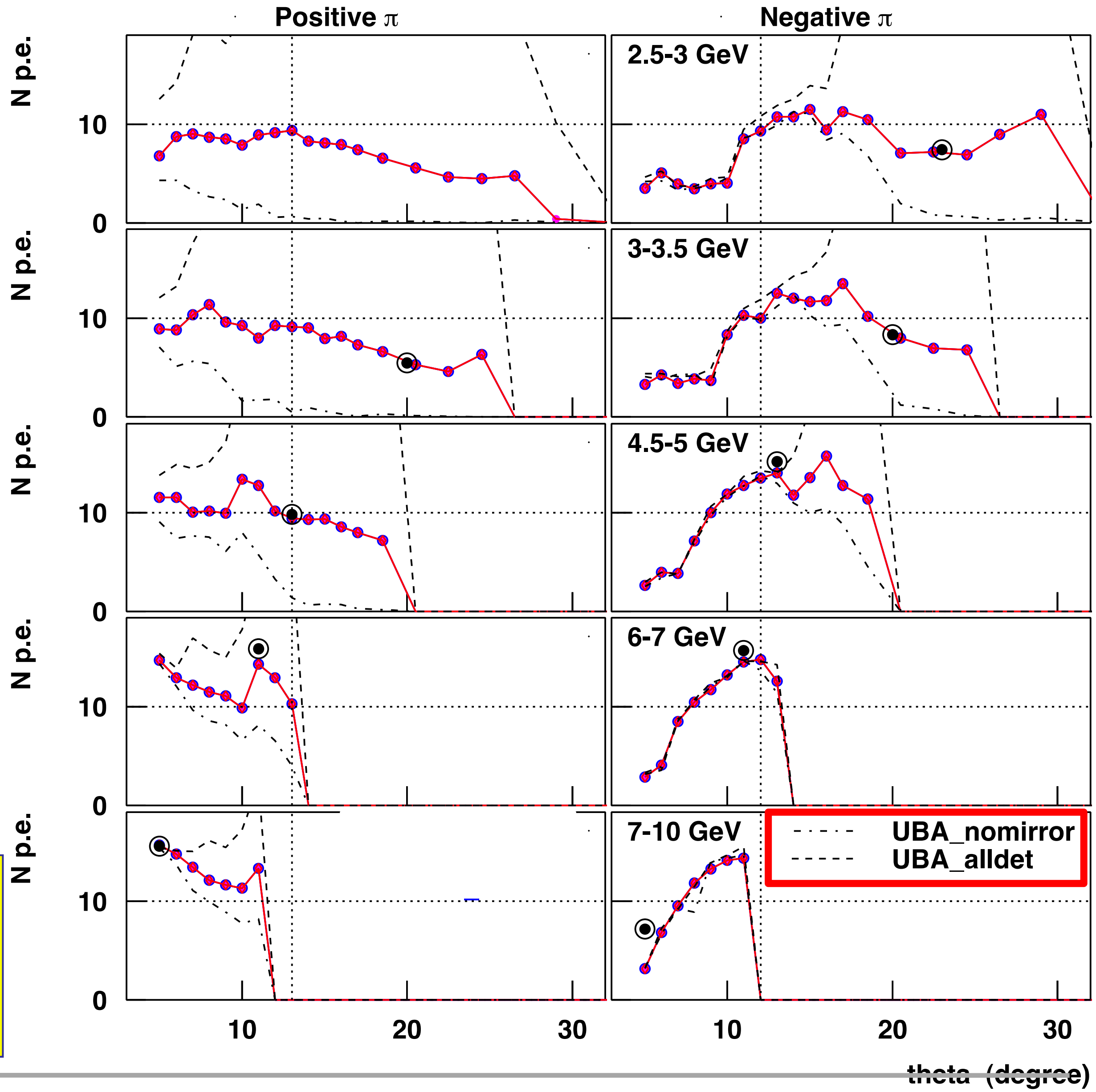

Average N p.e. : Mirror 14-25º PMTs: UBA

200 trials per point

Aerogel:

- n=1.06
- thick. increasing with radius: 2-4-6-8-10 cm

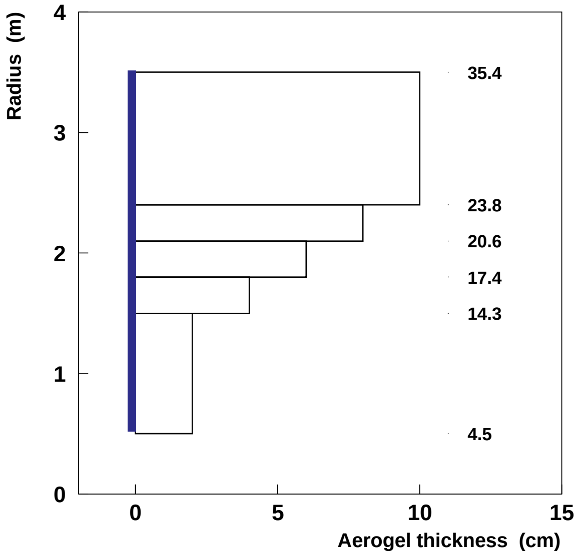

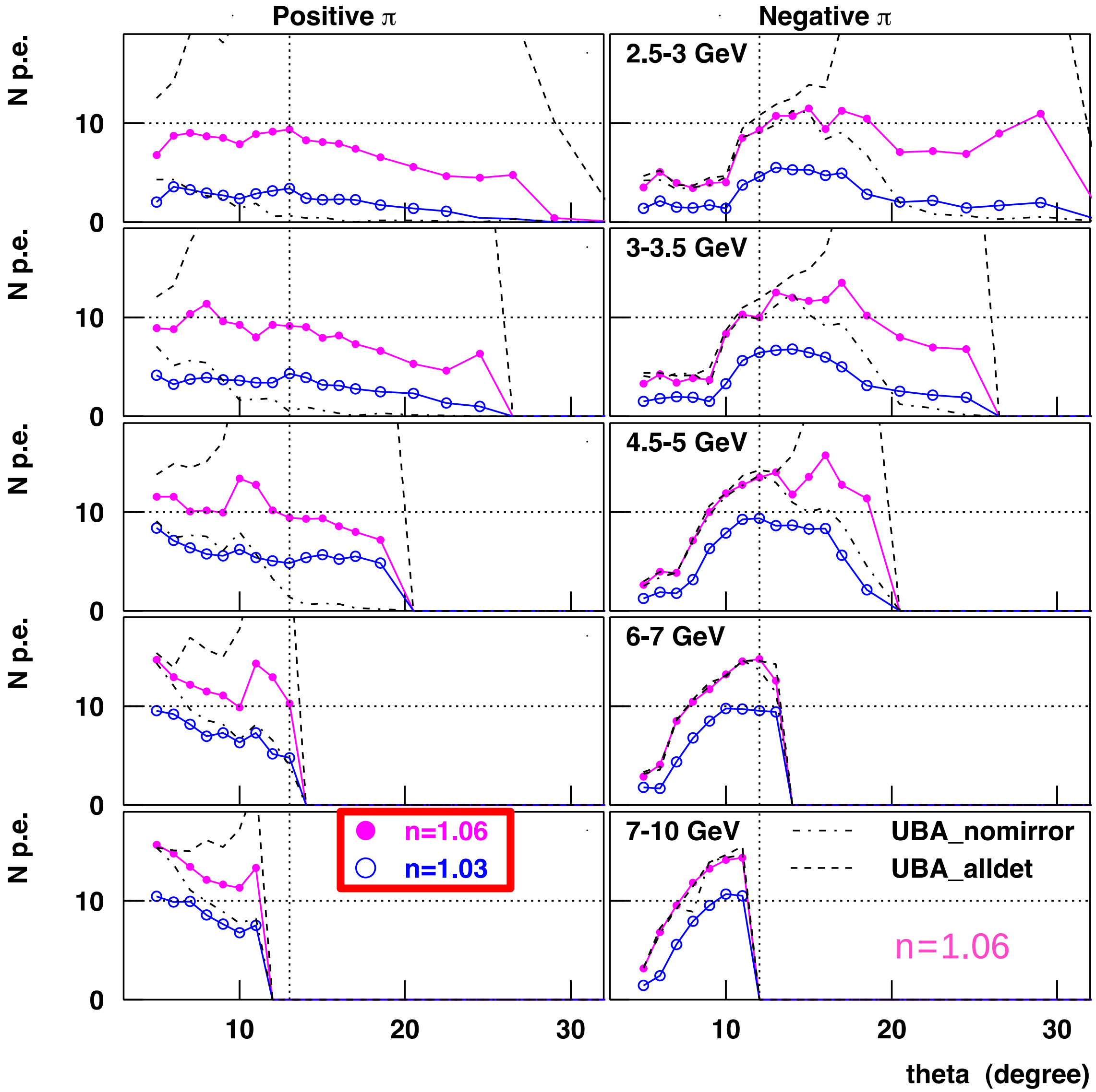

n=1.06 better for patter recognition in the presence of backgrouns

Average N p.e. : Mirror 14-25°

200 trials per point

Aerogel:

- n=1.06
- thick. increasing with radius: 2-4-6-8-10 cm

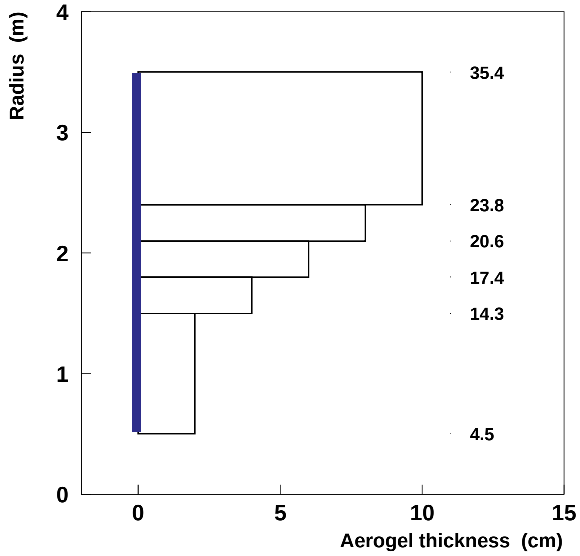

At least SBA PMTs are needed

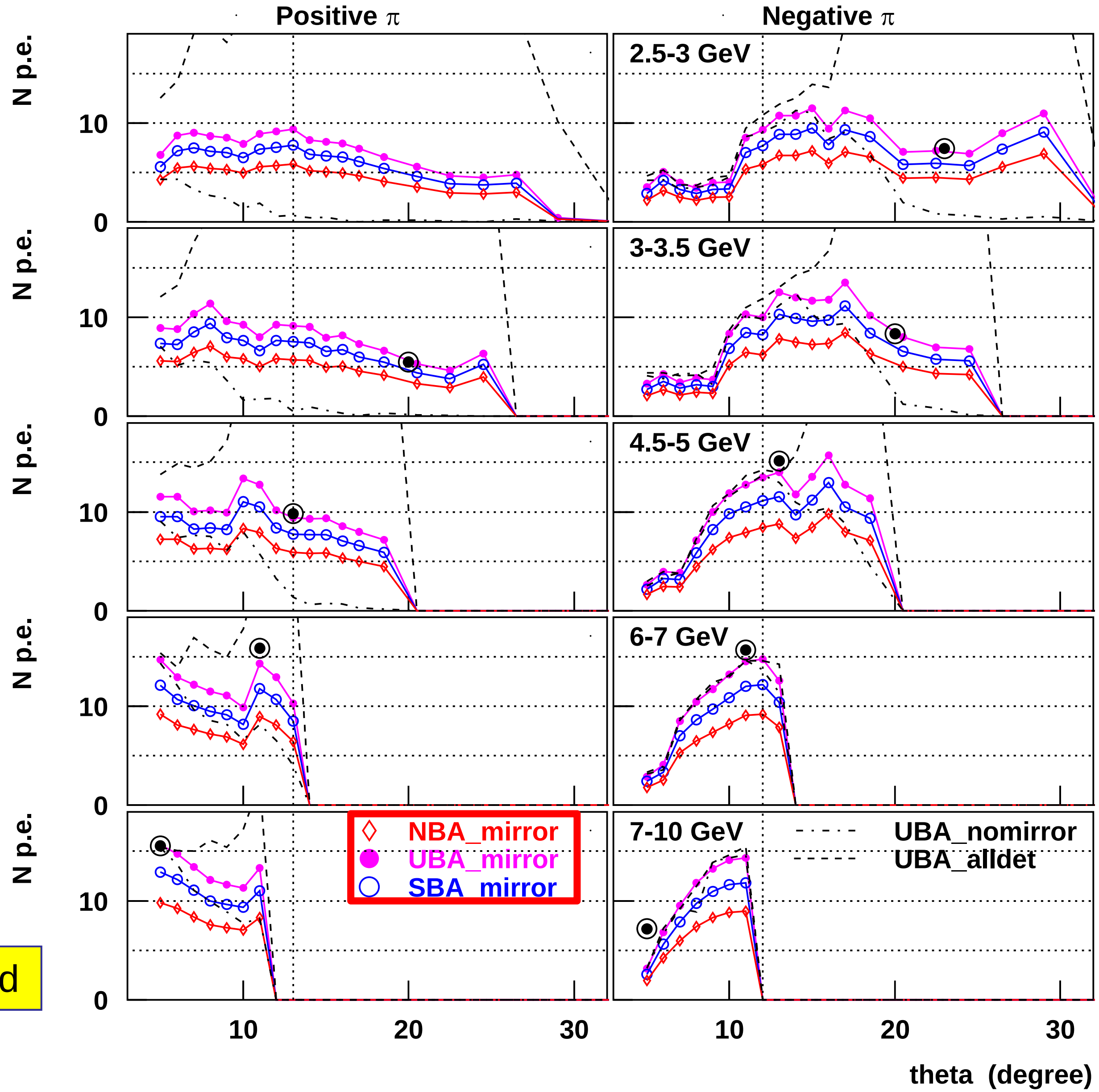

Average N p.e. : PMTs: UBA

200 trials per point

Aerogel:

- n=1.06
- thick. increasing with radius: 2-4-6-8-10 cm

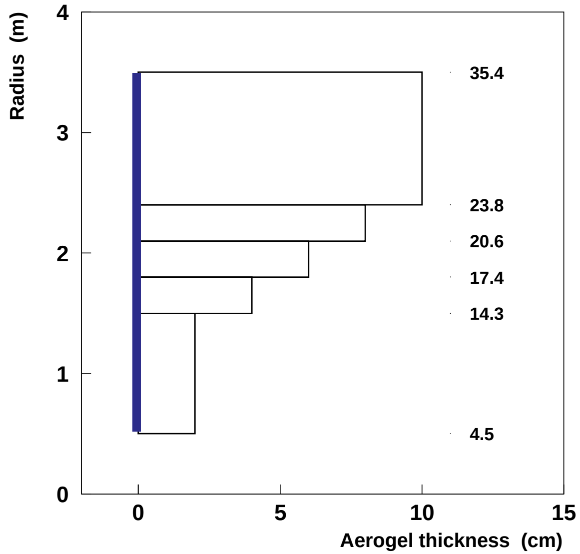

Mirror up to 35°:
Worse for positive hadrons
Better for negative hadrons

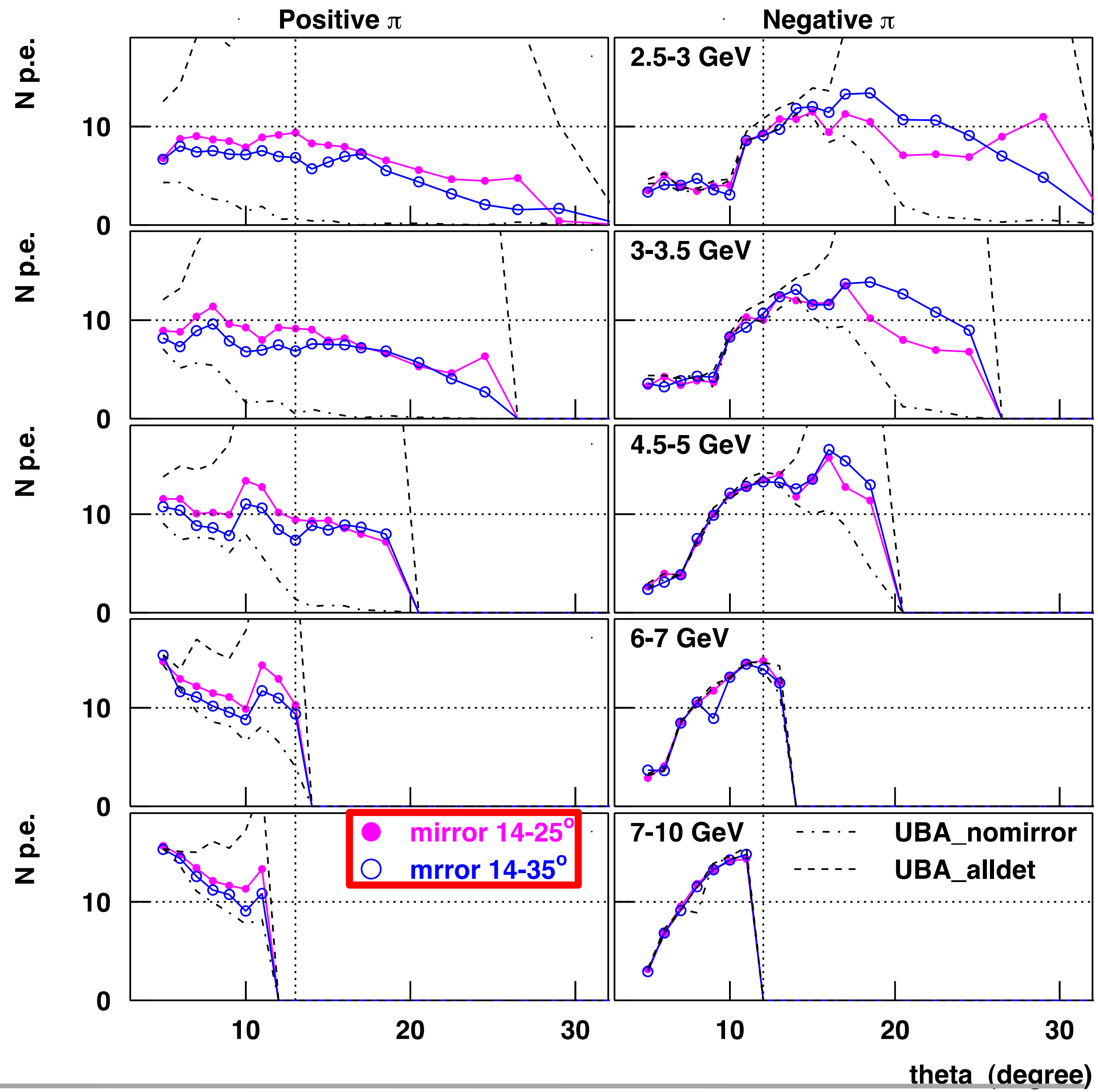

Average N p.e. : Aerogel thickness (UBA)

Mirror 14-35
PMT: UBA
100 trials per point

Aerogel:
- n=1.06

- thick. increasing with radius:
  2-4-6-8-10 cm
  2-2-10-10-10 cm
  3-5-5-10-10 cm

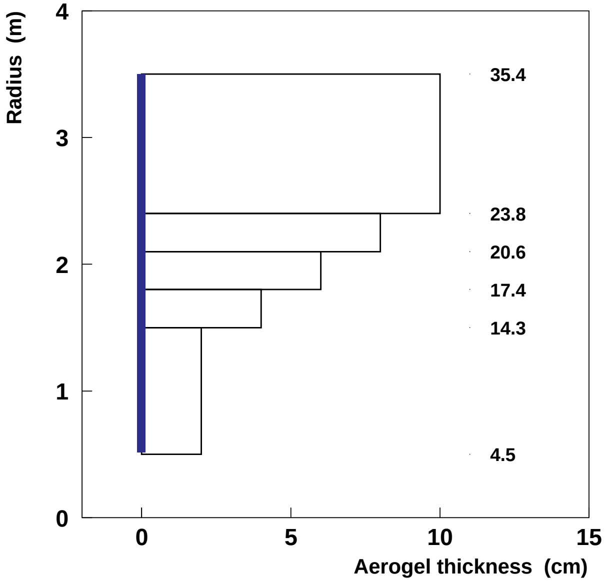

With 2-10 middle-angles improve
With 3-10 only small angles improve

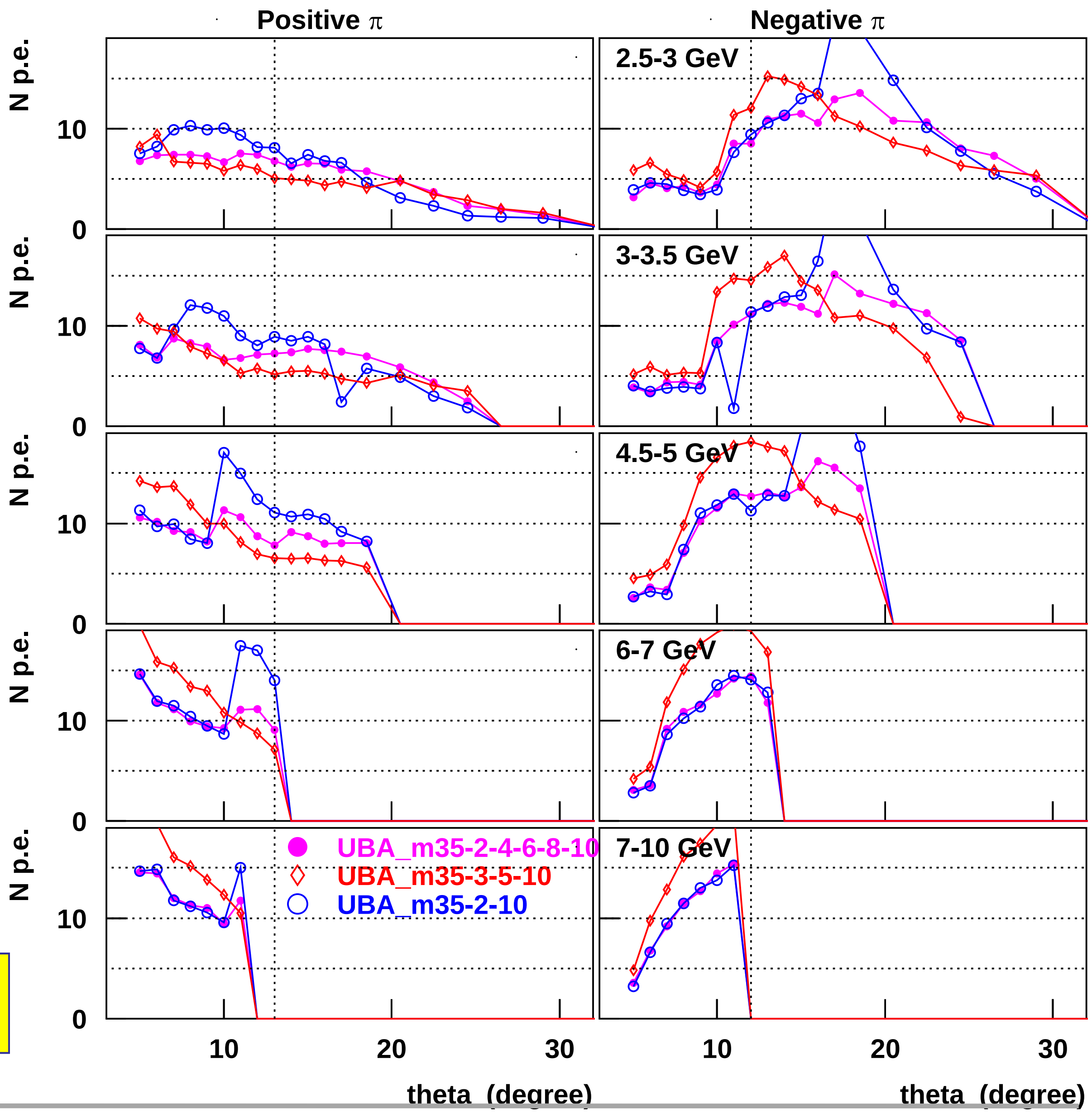

Average N p.e. : Semi-reflective Mirror (UBA)

Mirror 14-35
PMT: UBA
100 trials per point
Aerogel:
- n=1.06
- thick. increasing with radius: 6-6-6-10-10 cm

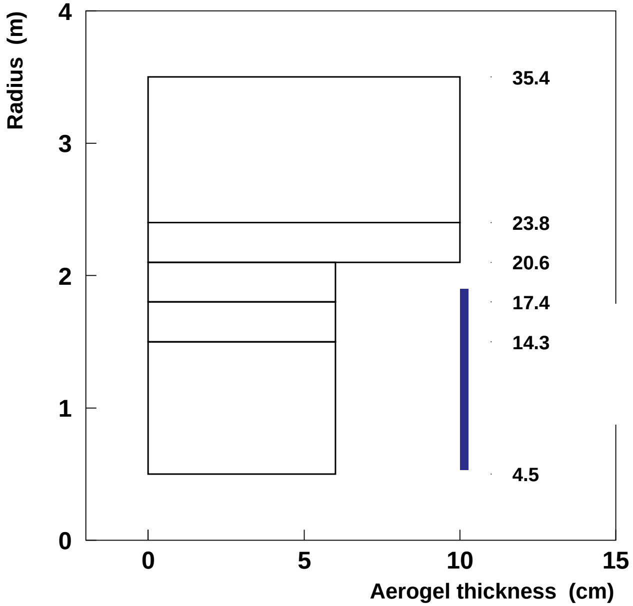

Same performance with Increased aerogel thickness

Can improve high angles only

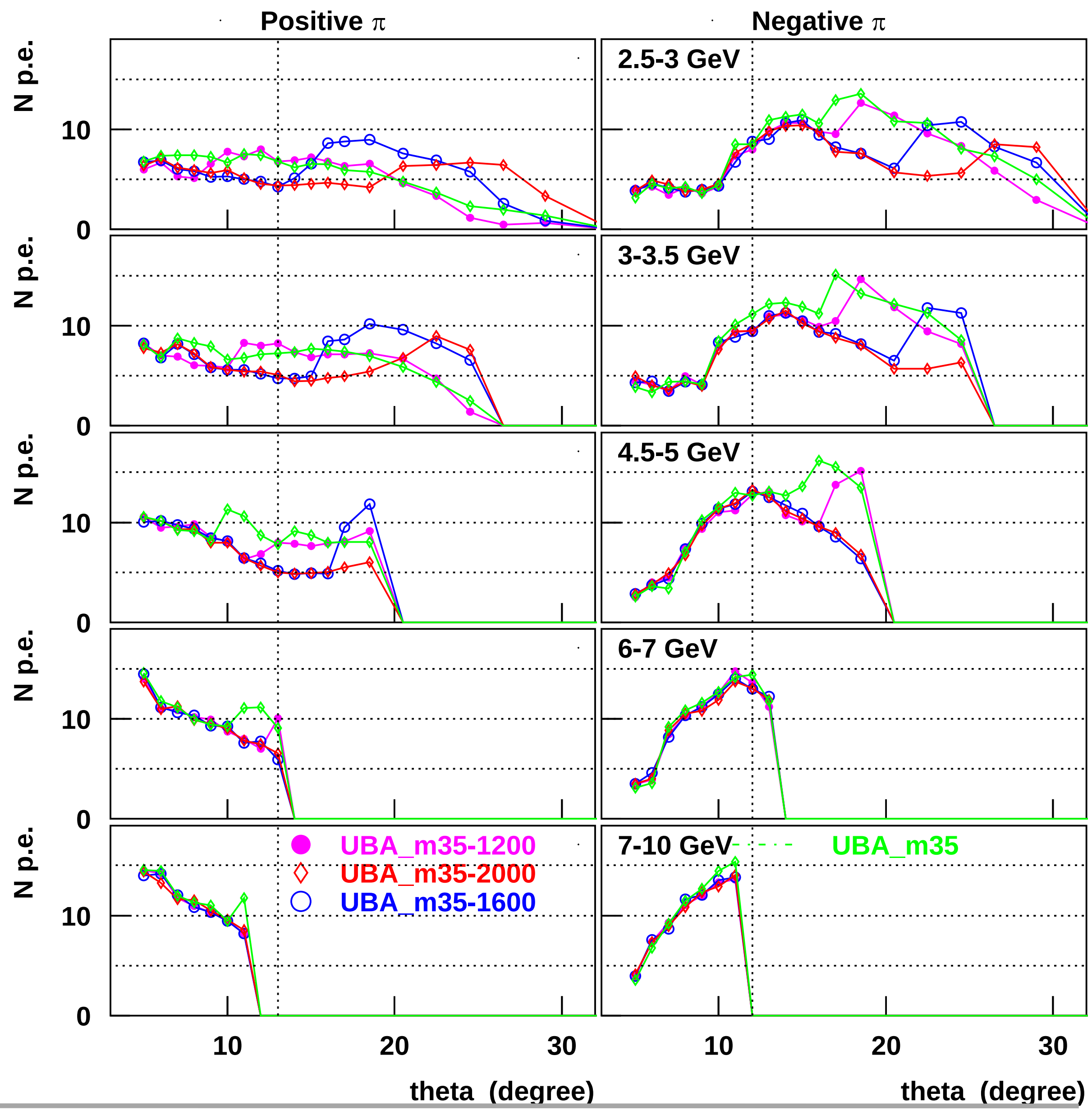

Conclusions

Aerogel provides a very good pion/kaon separation up to 8 GeV/c

• **Systematic studies performed with a GEANT3-based simulation provided an optimal configuration for the RICH in terms of pions/kaons separation**

• **RICH simulation is now being performed with GEMC (GEANT4-based)**
- realistic geometry
- realistic optical effects
- mirror system (different geometries tested)
- joint sectors
- multi-aerogel thickness
- semi-reflective plane mirror

• ***A new reconstruction algorithm allows for quantitative studies:***
n of p.e. for different configurations (studies ongoing)
π/K separation (next future)

Experiment proposals for CLAS12
(PAC38)

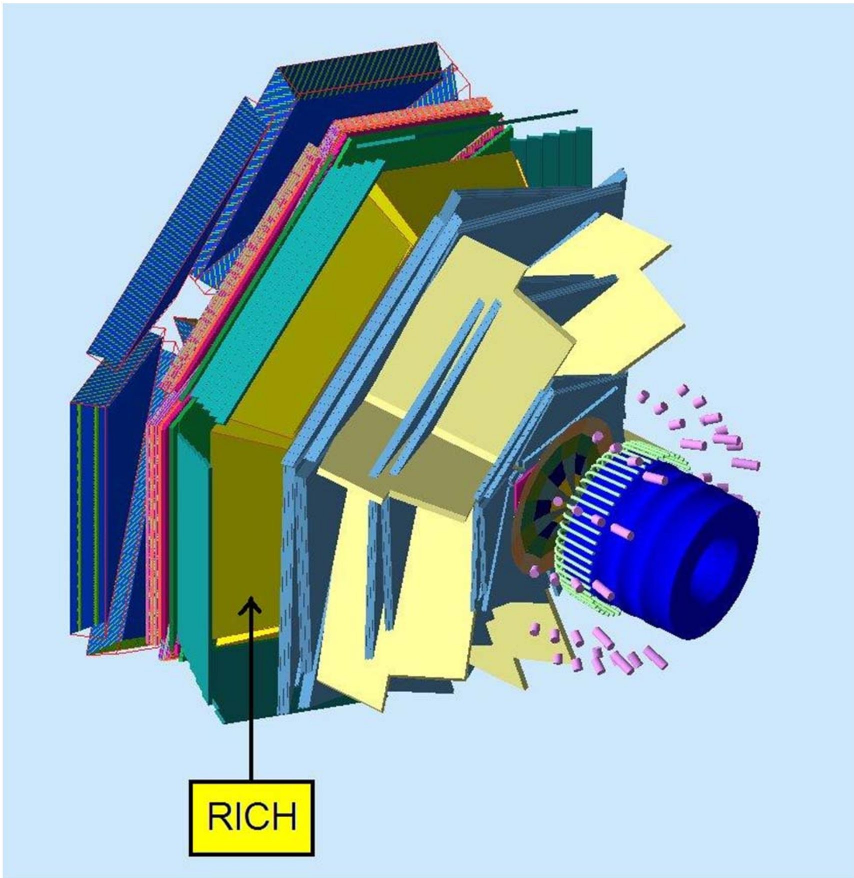

Experiment proposals for CLAS12 (PAC38)

Studies of Dihadron Electroproduction in DIS with Unpolarized and Longitudinally Polarized Hydrogen and Deuterium Targets

A CLAS collaboration proposal

H. Avakian (JLab), K. Griffioen (W&M), L.L. Pappalardo (Ferrara U.),
S. Pereira (LNF-INFN) A. Courtoy(Pavia U.)
* Contact: Harut Avakian, JLab, Newport News VA 23606. Email: avakian@jlab.org

Abstract

We are proposing a comprehensive program to study quark gluon correlations in semi-inclusive electroproduction of hadron pairs using the upgraded JLab 11 GeV polarized electron beam and the CLAS12 detector with unpolarized and longitudinally polarized proton and deuteron targets. The large acceptance of CLAS12 would allow simultaneous detection of the scattered electrons and hadrons from the hadronization of the struck quarks and target fragments, providing information on flavor and transverse momentum of underlying distribution functions. Pairs of hadrons detected in current fragmentation region would allow studies of higher twist distribution functions describing quark-gluon correlations, and chiral-odd Dihadron Fragmentation Functions (DiFF) describing correlations between the transverse polarization of the fragmenting quark with certain flavor and the azimuthal orientation of the plain containing the momenta of the detected hadron pair.

The study of processes with two hadron production – first in the current fragmentation region (CFR) and second in the target fragmentation region (TFR) – of polarized SIDIS provide complementary information on the nucleon structure and hadronization dynamics. The leading order azimuthal asymmetries in particular provide access to polarized TMD Fracture Functions, which are conditional probabilities to produce a hadron h in TFR when hard scattering occurs on quark q from the target nucleon N. For these processes for longitudinally polarized lepton scattering the cross-section depends on initial quark longitudinal polarization even if one does not measure the final quark polarization already in leading order.

The $x, z, P_T, M_{h,h}$ and Q^2 dependences of the $\sin\phi$ moments for CFR and TFR regions will be studied to probe the underlying distribution and fragmentation functions. Studies with kaons, enabled by the CLAS12 RICH detector, which are complementary to measurements with pions, will provide additional information on the corresponding structure functions.

The experiment will use the upgraded CLAS12 detector, 11 GeV highly polarized electron beam and unpolarized hydrogen and deuterium as well as longitudinally polarized solid ammonia targets (NH_3 and ND_3). We request 56 days of running on unpolarized hydrogen and deuterium and additional 30 days of running on NH_3 and 50

Studies of pion and kaon Electroproduction in semi-inclusive DIS with Transversely Polarized Hydrogen and Deuterium Targets

A CLAS collaboration proposal

M. Aghasyan (Frascati), H. Avakian (JLab), M. Contalbrigo* (Ferrara),
K. Joo (UConn), F.J. Klein (CUA)
* Contact: M. Contalbrigo, INFN-Ferrara, Email: contalbrigo@fe.infn.it

Abstract

We propose to study the azimuthal spin asymmetries in semi-inclusive DIS (SIDIS) with the CLAS12 spectrometer completed with a RICH detector, using the upgraded JLab 11 GeV polarized electron beam with transversely polarized proton and deuteron targets. The Fourier decomposition of the transverse-polarization-dependent cross-section term of the reaction $ep^{\uparrow} \rightarrow ehX$ (with h=π, K) provides access to a variety of fundamental quark correlation functions probing the parton dynamics within the nucleon and in the fragmentation process. Among them is the poorly known transversity function, whose precise measurement represents the missing piece for the full comprehension of the collinear structure of the nucleon at leading-twist. It differs from the helicity distribution due to the relativistic effects of the quark motion within the nucleon. Other prominent examples are the Sivers and Pretzelosity transverse-momentum-dependent (TMD) quark distributions. The Sivers function is related to the quark orbital motion in a transversely polarized nucleon and, being naive-T-odd, undergoes peculiar universality properties whose experimental verification is considered a key validation of the TMDs formalism. The Pretzelosity distribution function is sensitive to the D-wave component and probes any non-spherical shape of the nucleon. The measurable azimuthal asymmetries, interpreted as transverse-momentum-convolutions of parton distribution and fragmentation functions in the TMDs formalism, are expected to be in the range 2-10% from leading order calculations, depending on the kinematics and on the model used for the predictions. Chirally-odd distribution functions can be studied in conjunction with the Collins fragmentation function, which describes spin-orbit effects in the fragmentation of transversely polarized quarks. Alternatively, the transversity distribution can be studied in a collinear approach in conjunction with a di-hadron interference fragmentation function.

Flavor sensitivity is achieved by the identification of the final-state hadron, in particular kaon mesons, and the use of hydrogen and deuteron nucleon targets. This will help to clarify the "kaon puzzle" for, e.g., asymmetries related to transversity in conjunction with the Collins fragmentation function. HERMES results indicate that the single-spin asymmetries for pions and kaons may be very different. The asymmetries for K^+ are found of the same sign of those of π^+, which is expected if the valence

The table of TMDs

momentum

helicity

transversity

		quark		
		U	L	T
nucleon	U	f_1		
	L		g_1 −	
	T			h_1 − −

The table of TMDs

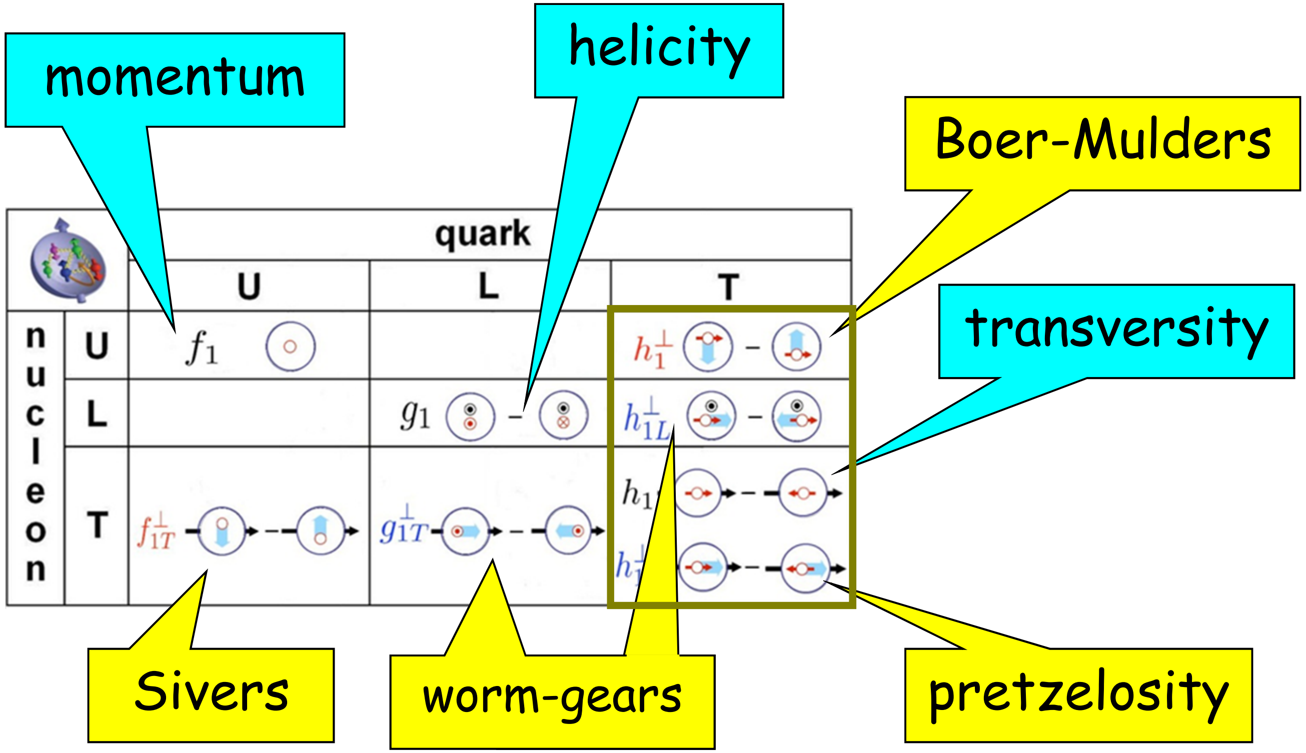

functions in red are naive T-odd

functions in green box are chirally odd

TMDs can be studied by measuring azimuthal asymmetries in SIDIS

Distribution Functions (DF)

nucleon		quark U	quark L	quark T
	U	f_1		$h_1^\perp$
	L		g_1	$h_{1L}^\perp$
	T	$f_{1T}^\perp$	$g_{1T}^\perp$	h_1, $h_{1T}^\perp$

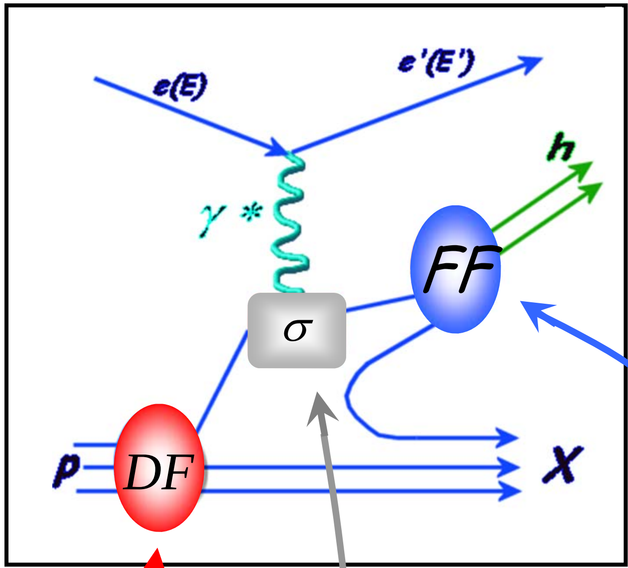

$$\sigma^{ep\to ehX} = \sum_q DF \otimes \sigma^{eq\to eq} \otimes FF$$

Fragmentation Functions (FF)

had.		quark U	quark L	quark T
	U	D_1 Unpol. FF		$H_1^\perp$ Collins FF

functions in red are naive T-odd

functions in green box are chirally odd

TMDs can be studied by measuring azimuthal asymmetries in SIDIS

Distribution Functions (DF)

nucleon \ quark	U	L	T
U	f_1		$h_1^\perp$
L		g_1	$h_{1L}^\perp$
T	$f_{1T}^\perp$	$g_{1T}^\perp$	h_1, $h_{1T}^\perp$

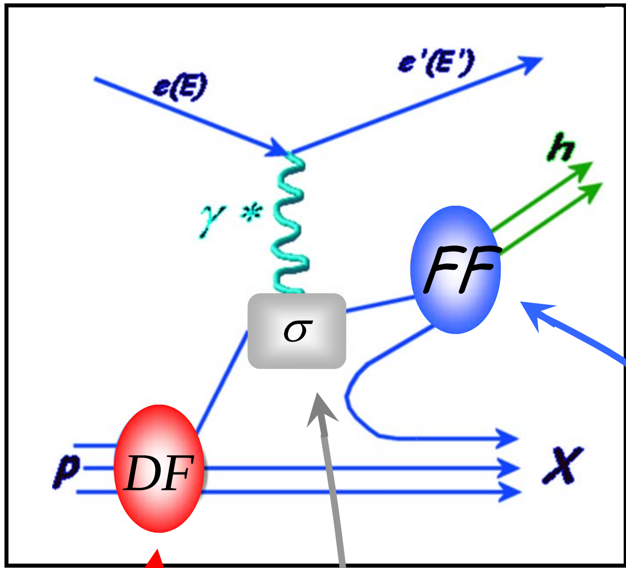

$$\sigma^{ep\to ehX} = \sum_q DF \otimes \sigma^{eq\to eq} \otimes FF$$

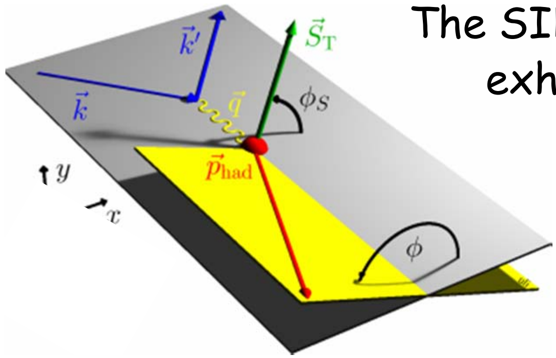

The SIDIS cross section exhibits asymmetries in the azimuthal angles ϕ and ϕ_S

Fragmentation Functions (FF)

had. \ quark	U	L	T
U	D_1 Unpol. FF		$H_1^\perp$ Collins FF

functions in red are naive T-odd

functions in green box are chirally odd

The SIDIS cross-section

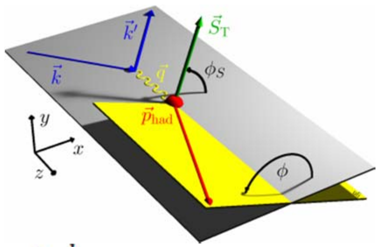

$$\frac{d\sigma^h}{dx\,dy\,d\phi_S\,dz\,d\phi\,d\mathbf{P}_{h\perp}^2} = \frac{\alpha^2}{xyQ^2}\frac{y^2}{2(1-\epsilon)}\left(1+\frac{\gamma^2}{2x}\right)$$

$$\Big\{ \Big[F_{UU,T} + \epsilon F_{UU,L} + \sqrt{2\epsilon(1+\epsilon)}\cos(\phi) F_{UU}^{\cos(\phi)} + \epsilon\cos(2\phi) F_{UU}^{\cos(2\phi)}\Big]$$

$$+ \lambda_l \Big[\sqrt{2\epsilon(1-\epsilon)}\sin(\phi) F_{LU}^{\sin(\phi)}\Big]$$

$$+ S_L \Big[\sqrt{2\epsilon(1+\epsilon)}\sin(\phi) F_{UL}^{\sin(\phi)} + \epsilon\sin(2\phi) F_{UL}^{\sin(2\phi)}\Big]$$

$$+ S_L\,\lambda_l \Big[\sqrt{1-\epsilon^2} F_{LL} + \sqrt{2\epsilon(1-\epsilon)}\cos(\phi) F_{LL}^{\cos(\phi)}\Big]$$

$$+ S_T \Big[\sin(\phi-\phi_S)\left(F_{UT,T}^{\sin(\phi-\phi_S)} + \epsilon F_{UT,L}^{\sin(\phi-\phi_S)}\right) + \epsilon\sin(\phi+\phi_S) F_{UT}^{\sin(\phi+\phi_S)} + \epsilon\sin(3\phi-\phi_S) F_{UT}^{\sin(3\phi-\phi_S)} + \sqrt{2\epsilon(1+\epsilon)}\sin(\phi_S) F_{UT}^{\sin(\phi_S)} + \sqrt{2\epsilon(1+\epsilon)}\sin(2\phi-\phi_S) F_{UT}^{\sin(2\phi-\phi_S)}\Big]$$

$$+ S_T\,\lambda_l \Big[\sqrt{1-\epsilon^2}\cos(\phi-\phi_S) F_{LT}^{\cos(\phi-\phi_S)} + \sqrt{2\epsilon(1-\epsilon)}\cos(\phi_S) F_{LT}^{\cos(\phi_S)} + \sqrt{2\epsilon(1-\epsilon)}\cos(2\phi-\phi_S) F_{LT}^{\cos(2\phi-\phi_S)}\Big]\Big\}$$

		quark		
		U	L	T
nucleon	U	f_1		$h_1^\perp$
	L		g_1	$h_{1L}^\perp$
	T	$f_{1T}^\perp$	$g_{1T}^\perp$	h_1 $h_{1T}^\perp$

The SIDIS cross-section

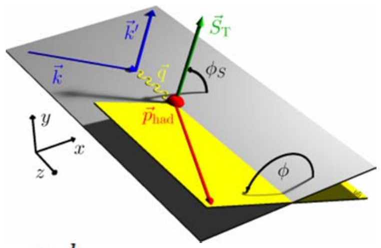

$$
\frac{d\sigma^h}{dx\,dy\,d\phi_S\,dz\,d\phi\,d\mathbf{P}_{h\perp}^2} = \frac{\alpha^2}{xyQ^2}\frac{y^2}{2(1-\epsilon)}\left(1+\frac{\gamma^2}{2x}\right)
$$

$$
\begin{aligned}
\Big\{ \quad & \Big[F_{\mathrm{UU,T}} + \epsilon F_{\mathrm{UU,L}} \\
& + \sqrt{2\epsilon(1+\epsilon)}\cos(\phi) F_{\mathrm{UU}}^{\cos(\phi)} + \epsilon\cos(2\phi) F_{\mathrm{UU}}^{\cos(2\phi)}\Big] \\
+ \quad \lambda_l \quad & \Big[\sqrt{2\epsilon(1-\epsilon)}\sin(\phi) F_{\mathrm{LU}}^{\sin(\phi)}\Big] \\
+ S_L \quad & \Big[\sqrt{2\epsilon(1+\epsilon)}\sin(\phi) F_{\mathrm{UL}}^{\sin(\phi)} + \epsilon\sin(2\phi) F_{\mathrm{UL}}^{\sin(2\phi)}\Big] \\
+ S_L\,\lambda_l \quad & \Big[\sqrt{1-\epsilon^2} F_{\mathrm{LL}} + \sqrt{2\epsilon(1-\epsilon)}\cos(\phi) F_{\mathrm{LL}}^{\cos(\phi)}\Big]
\end{aligned}
$$

$$
\begin{aligned}
+ S_T \quad & \Big[\sin(\phi-\phi_S)\left(F_{\mathrm{UT,T}}^{\sin(\phi-\phi_S)} + \epsilon F_{\mathrm{UT,L}}^{\sin(\phi-\phi_S)}\right) \\
& + \epsilon\sin(\phi+\phi_S) F_{\mathrm{UT}}^{\sin(\phi+\phi_S)} + \epsilon\sin(3\phi-\phi_S) F_{\mathrm{UT}}^{\sin(3\phi-\phi_S)} \\
& + \sqrt{2\epsilon(1+\epsilon)}\sin(\phi_S) F_{\mathrm{UT}}^{\sin(\phi_S)} \\
& + \sqrt{2\epsilon(1+\epsilon)}\sin(2\phi-\phi_S) F_{\mathrm{UT}}^{\sin(2\phi-\phi_S)}\Big] \\
+ S_T\,\lambda_l \quad & \Big[\sqrt{1-\epsilon^2}\cos(\phi-\phi_S) F_{\mathrm{LT}}^{\cos(\phi-\phi_S)} \\
& + \sqrt{2\epsilon(1-\epsilon)}\cos(\phi_S) F_{\mathrm{LT}}^{\cos(\phi_S)} \\
& + \sqrt{2\epsilon(1-\epsilon)}\cos(2\phi-\phi_S) F_{\mathrm{LT}}^{\cos(2\phi-\phi_S)}\Big]\Big\}
\end{aligned}
$$

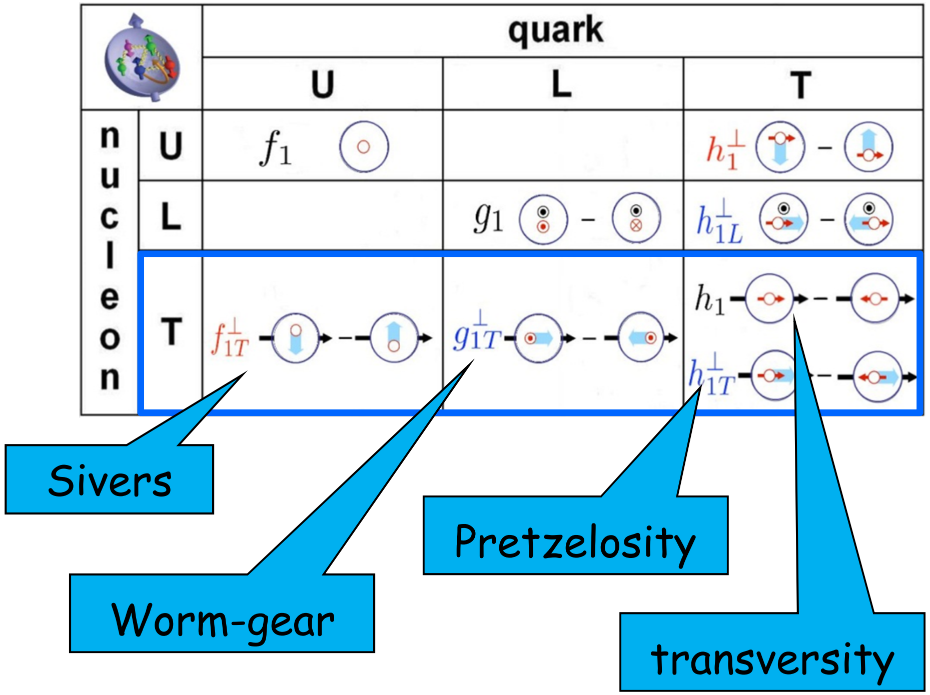

The Collins effect

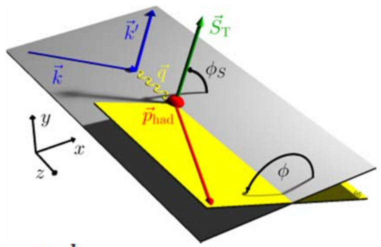

$$
\begin{aligned}
\frac{d\sigma^h}{dx\,dy\,d\phi_S\,dz\,d\phi\,d\mathbf{P}_{h\perp}^2} = & \frac{\alpha^2}{xyQ^2}\frac{y^2}{2(1-\epsilon)}\left(1+\frac{\gamma^2}{2x}\right) \\
\Bigg\{ & \Big[F_{\mathrm{UU,T}} + \epsilon F_{\mathrm{UU,L}} \\
& +\sqrt{2\epsilon(1+\epsilon)}\cos(\phi) F_{\mathrm{UU}}^{\cos(\phi)} + \epsilon\cos(2\phi) F_{\mathrm{UU}}^{\cos(2\phi)}\Big] \\
+ \quad \lambda_l & \Big[\sqrt{2\epsilon(1-\epsilon)}\sin(\phi) F_{\mathrm{LU}}^{\sin(\phi)}\Big] \\
+ S_L \quad & \Big[\sqrt{2\epsilon(1+\epsilon)}\sin(\phi) F_{\mathrm{UL}}^{\sin(\phi)} + \epsilon\sin(2\phi) F_{\mathrm{UL}}^{\sin(2\phi)}\Big] \\
+ S_L\ \lambda_l & \Big[\sqrt{1-\epsilon^2} F_{\mathrm{LL}} + \sqrt{2\epsilon(1-\epsilon)}\cos(\phi) F_{\mathrm{LL}}^{\cos(\phi)}\Big] \\
+ S_T \quad & \Big[\sin(\phi-\phi_S)\left(F_{\mathrm{UT,T}}^{\sin(\phi-\phi_S)} + \epsilon F_{\mathrm{UT,L}}^{\sin(\phi-\phi_S)}\right) \\
& +\epsilon\sin(\phi+\phi_S) F_{\mathrm{UT}}^{\sin(\phi+\phi_S)} + \epsilon\sin(3\phi-\phi_S) F_{\mathrm{UT}}^{\sin(3\phi-\phi_S)} \\
& +\sqrt{2\epsilon(1+\epsilon)}\sin(\phi_S) F_{\mathrm{UT}}^{\sin(\phi_S)} \\
& +\sqrt{2\epsilon(1+\epsilon)}\sin(2\phi-\phi_S) F_{\mathrm{UT}}^{\sin(2\phi-\phi_S)}\Big] \\
+ S_T\ \lambda_l & \Big[\sqrt{1-\epsilon^2}\cos(\phi-\phi_S) F_{\mathrm{LT}}^{\cos(\phi-\phi_S)} \\
& +\sqrt{2\epsilon(1-\epsilon)}\cos(\phi_S) F_{\mathrm{LT}}^{\cos(\phi_S)} \\
& +\sqrt{2\epsilon(1-\epsilon)}\cos(2\phi-\phi_S) F_{\mathrm{LT}}^{\cos(2\phi-\phi_S)}\Big]\Bigg\}
\end{aligned}
$$

		quark		
		U	L	T
nucleon	U	f_1		$h_1^\perp$
	L		g_1	$h_{1L}^\perp$
	T	$f_{1T}^\perp$	$g_{1T}^\perp$	h_1, $h_{1T}^\perp$

Collins effect

- $\propto h_1(x, p_T^2) \otimes H_1^\perp(z, k_T^2)$
- correlation between parton transverse polarization in a transversely polarized nucleon and transverse momentum of the produced hadron

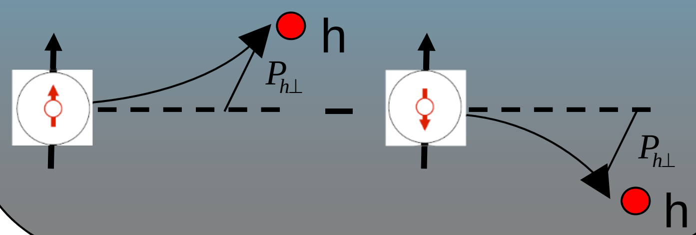

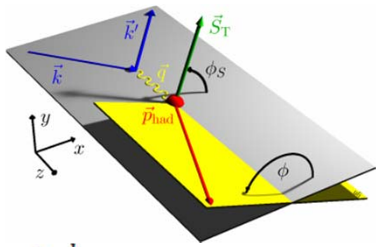

The Sivers effect

$$
\begin{aligned}
\frac{d\sigma^h}{dx\,dy\,d\phi_S\,dz\,d\phi\,d\mathbf{P}^2_{h\perp}} = {} & \frac{\alpha^2}{xyQ^2}\frac{y^2}{2(1-\epsilon)}\left(1+\frac{\gamma^2}{2x}\right) \\
\Big\{ & \Big[F_{\mathrm{UU,T}}+\epsilon F_{\mathrm{UU,L}} \\
& +\sqrt{2\epsilon(1+\epsilon)}\cos(\phi)F_{\mathrm{UU}}^{\cos(\phi)}+\epsilon\cos(2\phi)F_{\mathrm{UU}}^{\cos(2\phi)}\Big] \\
+ \quad & \lambda_l\Big[\sqrt{2\epsilon(1-\epsilon)}\sin(\phi)F_{\mathrm{LU}}^{\sin(\phi)}\Big] \\
+ S_L \quad & \Big[\sqrt{2\epsilon(1+\epsilon)}\sin(\phi)F_{\mathrm{UL}}^{\sin(\phi)}+\epsilon\sin(2\phi)F_{\mathrm{UL}}^{\sin(2\phi)}\Big] \\
+ S_L\ \lambda_l & \Big[\sqrt{1-\epsilon^2}F_{\mathrm{LL}}+\sqrt{2\epsilon(1-\epsilon)}\cos(\phi)F_{\mathrm{LL}}^{\cos(\phi)}\Big] \\
+ S_T \quad & \Big[\sin(\phi-\phi_S)\left(F_{\mathrm{UT,T}}^{\sin(\phi-\phi_S)}+\epsilon F_{\mathrm{UT,L}}^{\sin(\phi-\phi_S)}\right) \\
& +\epsilon\sin(\phi+\phi_S)F_{\mathrm{UT}}^{\sin(\phi+\phi_S)}+\epsilon\sin(3\phi-\phi_S)F_{\mathrm{UT}}^{\sin(3\phi-\phi_S)} \\
& +\sqrt{2\epsilon(1+\epsilon)}\sin(\phi_S)F_{\mathrm{UT}}^{\sin(\phi_S)} \\
& +\sqrt{2\epsilon(1+\epsilon)}\sin(2\phi-\phi_S)F_{\mathrm{UT}}^{\sin(2\phi-\phi_S)}\Big] \\
+ S_T\ \lambda_l & \Big[\sqrt{1-\epsilon^2}\cos(\phi-\phi_S)F_{\mathrm{LT}}^{\cos(\phi-\phi_S)} \\
& +\sqrt{2\epsilon(1-\epsilon)}\cos(\phi_S)F_{\mathrm{LT}}^{\cos(\phi_S)} \\
& +\sqrt{2\epsilon(1-\epsilon)}\cos(2\phi-\phi_S)F_{\mathrm{LT}}^{\cos(2\phi-\phi_S)}\Big]\Big\}
\end{aligned}
$$

		quark		
		U	L	T
nucleon	U	f_1		$h_1^\perp$ -
	L		g_1 -	$h_{1L}^\perp$ -
	T	$f_{1T}^\perp$ -	$g_{1T}^\perp$ -	h_1 - $h_{1T}^\perp$ -

Sivers effect

$$\propto f_{1T}^\perp(x, p_T^2) \otimes D_1(z, k_T^2)$$

- correlation between parton transverse momentum and nucleon transverse polarization
- requires orbital angular momentum

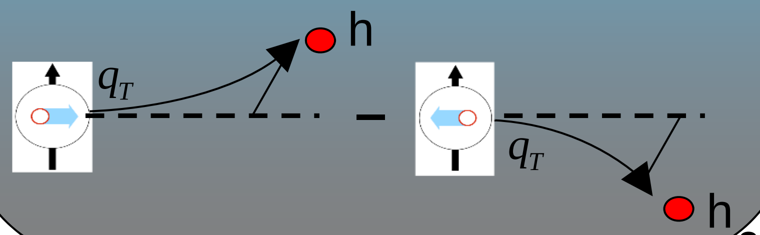

The "pretzelosity"

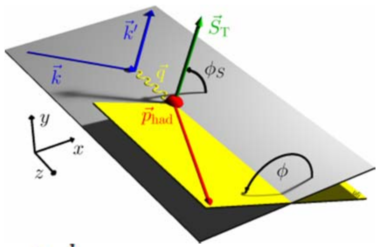

$$
\frac{d\sigma^h}{dx\,dy\,d\phi_S\,dz\,d\phi\,d\mathbf{P}_{h\perp}^2} = \frac{\alpha^2}{xyQ^2}\frac{y^2}{2(1-\epsilon)}\left(1+\frac{\gamma^2}{2x}\right)
$$

$$
\begin{aligned}
\Big\{ \quad & \Big[F_{\rm UU,T} + \epsilon F_{\rm UU,L} \\
& + \sqrt{2\epsilon(1+\epsilon)}\cos(\phi) F_{\rm UU}^{\cos(\phi)} + \epsilon\cos(2\phi) F_{\rm UU}^{\cos(2\phi)}\Big] \\
+ \quad \lambda_l \ & \Big[\sqrt{2\epsilon(1-\epsilon)}\sin(\phi) F_{\rm LU}^{\sin(\phi)}\Big] \\
+ \ S_L \ & \Big[\sqrt{2\epsilon(1+\epsilon)}\sin(\phi) F_{\rm UL}^{\sin(\phi)} + \epsilon\sin(2\phi) F_{\rm UL}^{\sin(2\phi)}\Big] \\
+ \ S_L\,\lambda_l \ & \Big[\sqrt{1-\epsilon^2} F_{\rm LL} + \sqrt{2\epsilon(1-\epsilon)}\cos(\phi) F_{\rm LL}^{\cos(\phi)}\Big] \\
+ \ S_T \ & \Big[\sin(\phi-\phi_S)\left(F_{\rm UT,T}^{\sin(\phi-\phi_S)} + \epsilon F_{\rm UT,L}^{\sin(\phi-\phi_S)}\right) \\
& + \epsilon\sin(\phi+\phi_S) F_{\rm UT}^{\sin(\phi+\phi_S)} + \boxed{\epsilon\sin(3\phi-\phi_S) F_{\rm UT}^{\sin(3\phi-\phi_S)}} \\
& + \sqrt{2\epsilon(1+\epsilon)}\sin(\phi_S) F_{\rm UT}^{\sin(\phi_S)} \\
& + \sqrt{2\epsilon(1+\epsilon)}\sin(2\phi-\phi_S) F_{\rm UT}^{\sin(2\phi-\phi_S)}\Big] \\
+ \ S_T\,\lambda_l \ & \Big[\sqrt{1-\epsilon^2}\cos(\phi-\phi_S) F_{\rm LT}^{\cos(\phi-\phi_S)} \\
& + \sqrt{2\epsilon(1-\epsilon)}\cos(\phi_S) F_{\rm LT}^{\cos(\phi_S)} \\
& + \sqrt{2\epsilon(1-\epsilon)}\cos(2\phi-\phi_S) F_{\rm LT}^{\cos(2\phi-\phi_S)}\Big]\Big\}
\end{aligned}
$$

		quark		
		U	L	T
nucleon	U	f_1		$h_1^\perp$
	L		g_1	$h_{1L}^\perp$
	T	$f_{1T}^\perp$	$g_{1T}^\perp$	h_1 $h_{1T}^\perp$

pretzelosity

$$\propto h_{1T}^\perp(x, p_T^2) \otimes H_1^\perp(z, k_T^2)$$

- correlation between the quark transverse momentum and the quark transverse spin within a transversely polarized nucleon
- can be linked to the non-spherical shape of the nucleon resulting from substantial quark orbital angular momentum

The worm-gear $g_{1T}{}^{\perp}$

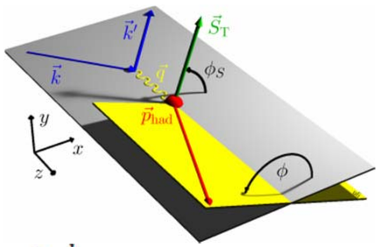

$$\frac{d\sigma^h}{dx\,dy\,d\phi_S\,dz\,d\phi\,d\mathbf{P}_{h\perp}^2} = \frac{\alpha^2}{xyQ^2}\frac{y^2}{2(1-\epsilon)}\left(1+\frac{\gamma^2}{2x}\right)$$

$$\Big\{ \Big[F_{UU,T} + \epsilon F_{UU,L} + \sqrt{2\epsilon(1+\epsilon)}\cos(\phi) F_{UU}^{\cos(\phi)} + \epsilon\cos(2\phi) F_{UU}^{\cos(2\phi)}\Big]$$

$$+ \lambda_l \Big[\sqrt{2\epsilon(1-\epsilon)}\sin(\phi) F_{LU}^{\sin(\phi)}\Big]$$

$$+ S_L \Big[\sqrt{2\epsilon(1+\epsilon)}\sin(\phi) F_{UL}^{\sin(\phi)} + \epsilon\sin(2\phi) F_{UL}^{\sin(2\phi)}\Big]$$

$$+ S_L\,\lambda_l \Big[\sqrt{1-\epsilon^2} F_{LL} + \sqrt{2\epsilon(1-\epsilon)}\cos(\phi) F_{LL}^{\cos(\phi)}\Big]$$

$$+ S_T \Big[\sin(\phi-\phi_S)\left(F_{UT,T}^{\sin(\phi-\phi_S)} + \epsilon F_{UT,L}^{\sin(\phi-\phi_S)}\right) + \epsilon\sin(\phi+\phi_S) F_{UT}^{\sin(\phi+\phi_S)} + \epsilon\sin(3\phi-\phi_S) F_{UT}^{\sin(3\phi-\phi_S)} + \sqrt{2\epsilon(1+\epsilon)}\sin(\phi_S) F_{UT}^{\sin(\phi_S)} + \sqrt{2\epsilon(1+\epsilon)}\sin(2\phi-\phi_S) F_{UT}^{\sin(2\phi-\phi_S)}\Big]$$

$$+ S_T\,\lambda_l \Big[\sqrt{1-\epsilon^2}\cos(\phi-\phi_S) F_{LT}^{\cos(\phi-\phi_S)} + \sqrt{2\epsilon(1-\epsilon)}\cos(\phi_S) F_{LT}^{\cos(\phi_S)} + \sqrt{2\epsilon(1-\epsilon)}\cos(2\phi-\phi_S) F_{LT}^{\cos(2\phi-\phi_S)}\Big]\Big\}$$

		quark		
		U	L	T
nucleon	U	f_1		$h_1^{\perp}$
	L		g_1	$h_{1L}^{\perp}$
	T	$f_{1T}^{\perp}$	$g_{1T}^{\perp}$	h_1, $h_{1T}^{\perp}$

Worm-gear

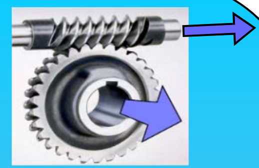

$$\propto g_{1T}^{\perp}(x, p_T^2) \otimes D_1(z, k_T^2)$$

- describes the probability to find longitudinally polarized quarks in a transversely polarized nucleon (→ "**trans-helicity**")
- accessible in LT DSAs through the leading-twist cos(ϕ-ϕ_S) Fourier component

1-dim projected results: Collins & Sivers

Beam request: 100 days
- 80 days of continuative measurements
- 20 days for calibrations, empty target runs, auxiliary tests

HD-Ice target
- H pol 75%, D pol 40%
- dilution (for H) ~ 1/3
- Compensation coil to cancel long. field from solenoid (simulations with TOSCA)

Kinematic cuts
- $Q^2 > 1\ GeV^2$ $(\rightarrow \mathrm{x} > 0.05)$
- $W^2 > 4\ GeV^2$
- $0.10 < y < 0.95$
- $0.2 < z < 0.7$
- π^0: $0.097 < m_{\gamma\gamma} < 0.179\ GeV/c^2$

Projections

HERMES model → CLAS12 MC

1-dim projected results: Collins & Sivers

Beam request: 100 days

- 80 days of continuative measurements
- 20 days for calibrations, empty target runs, auxiliary tests

HD-Ice target

- H pol 75%, D pol 40%
- dilution (for H) ~ 1/3
- Compensation coil to cancel long. field from solenoid (simulations with TOSCA)

Kinematic cuts

- $Q^2 > 1\,GeV^2$ $(\rightarrow x > 0.05)$
- $W^2 > 4\,GeV^2$
- $0.10 < y < 0.95$
- $0.2 < z < 0.7$
- π^0: $0.097 < m_{\gamma\gamma} < 0.179\,GeV/c^2$

Projections

HERMES model → CLAS12 MC

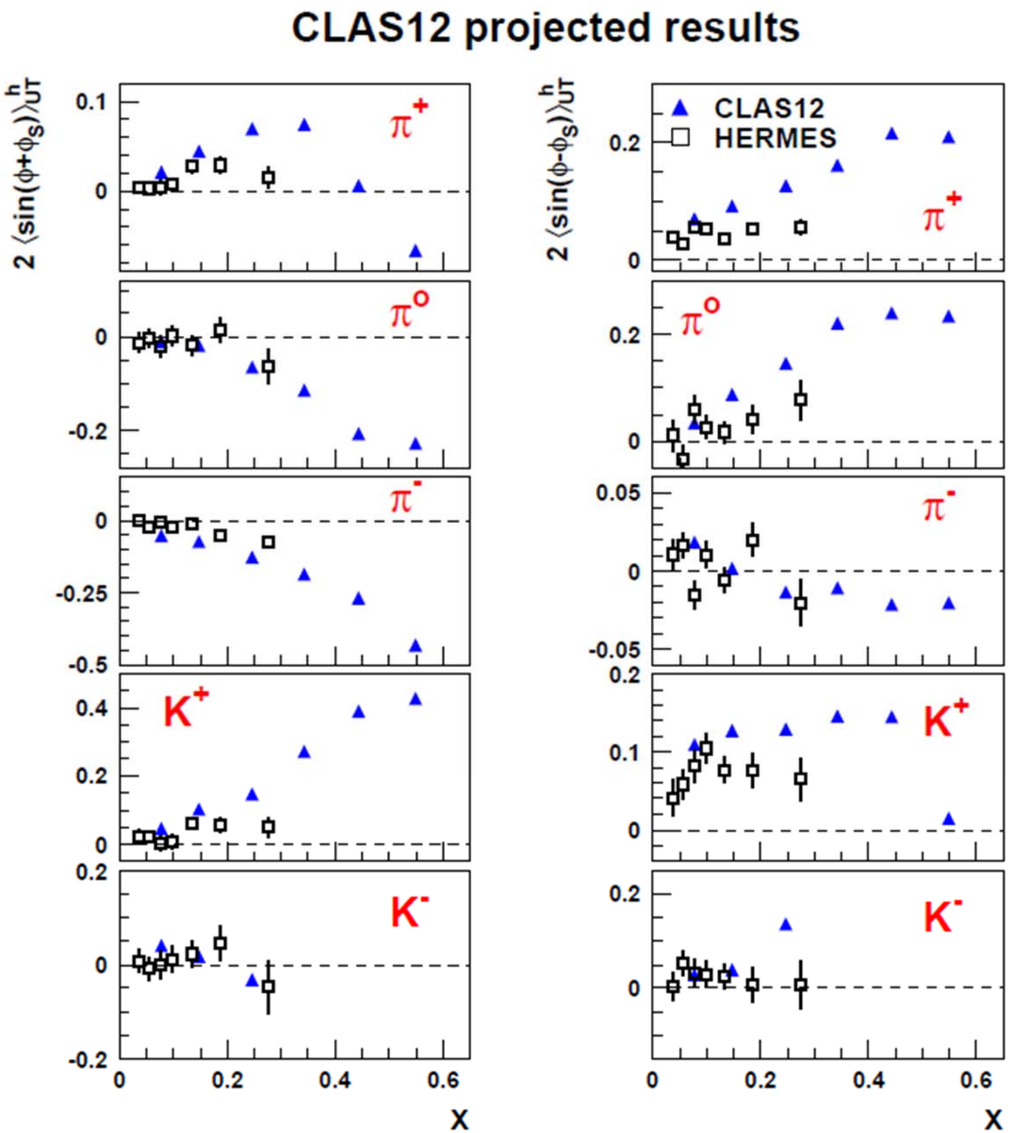

Extracted amplitudes are only indicative, but statistical precision is realistic

2-dim projected results: Collins & Sivers

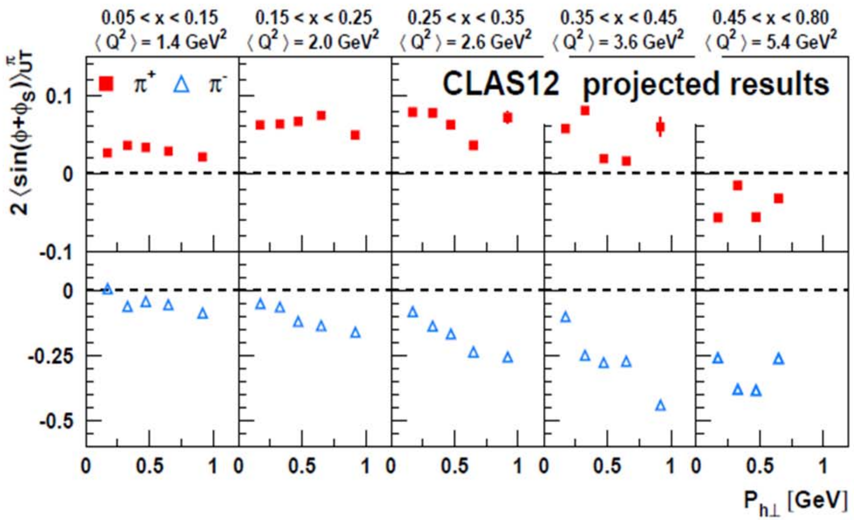

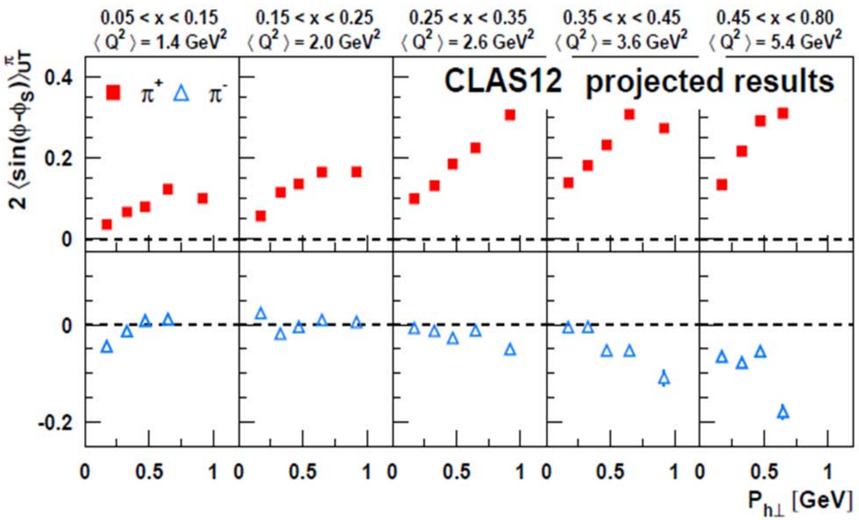

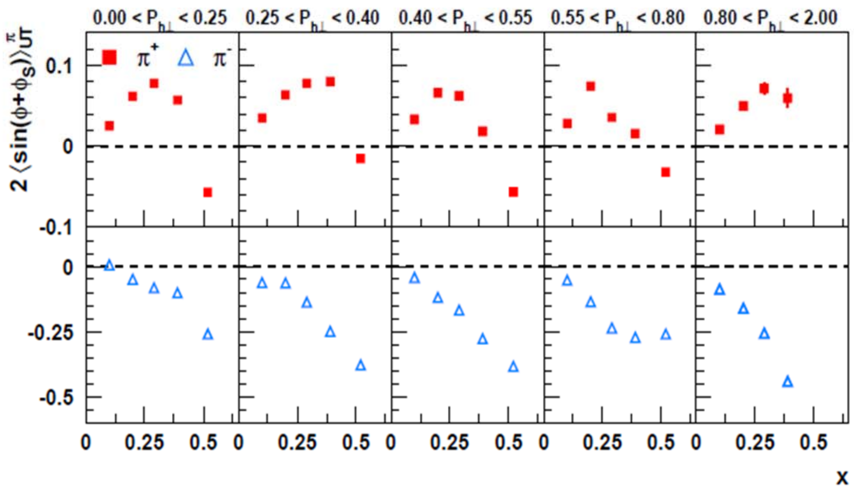

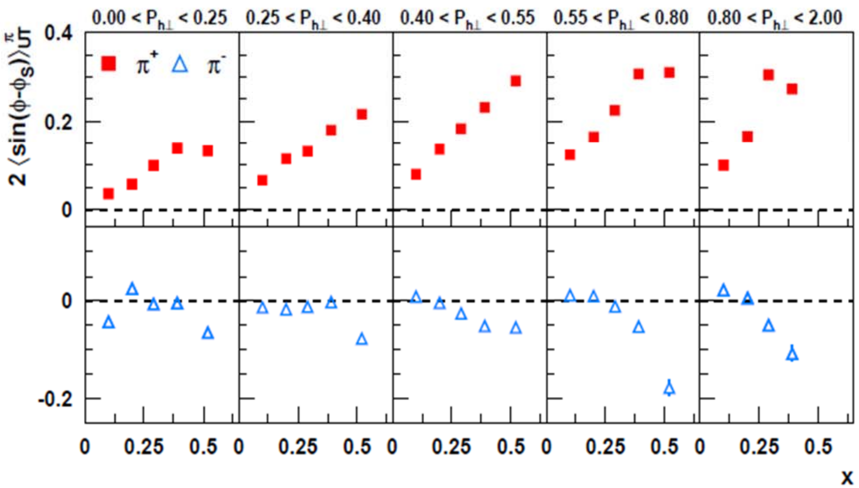

Extracted amplitudes are only indicative, but statistical precision is realistic

Magnetic field design (M. Statera)

Magnetic field simulations by TOSCA:

- main solenoid (5 T)
- correction solenoid

create a zero field region

- insert a simple dipole saddle (1T)

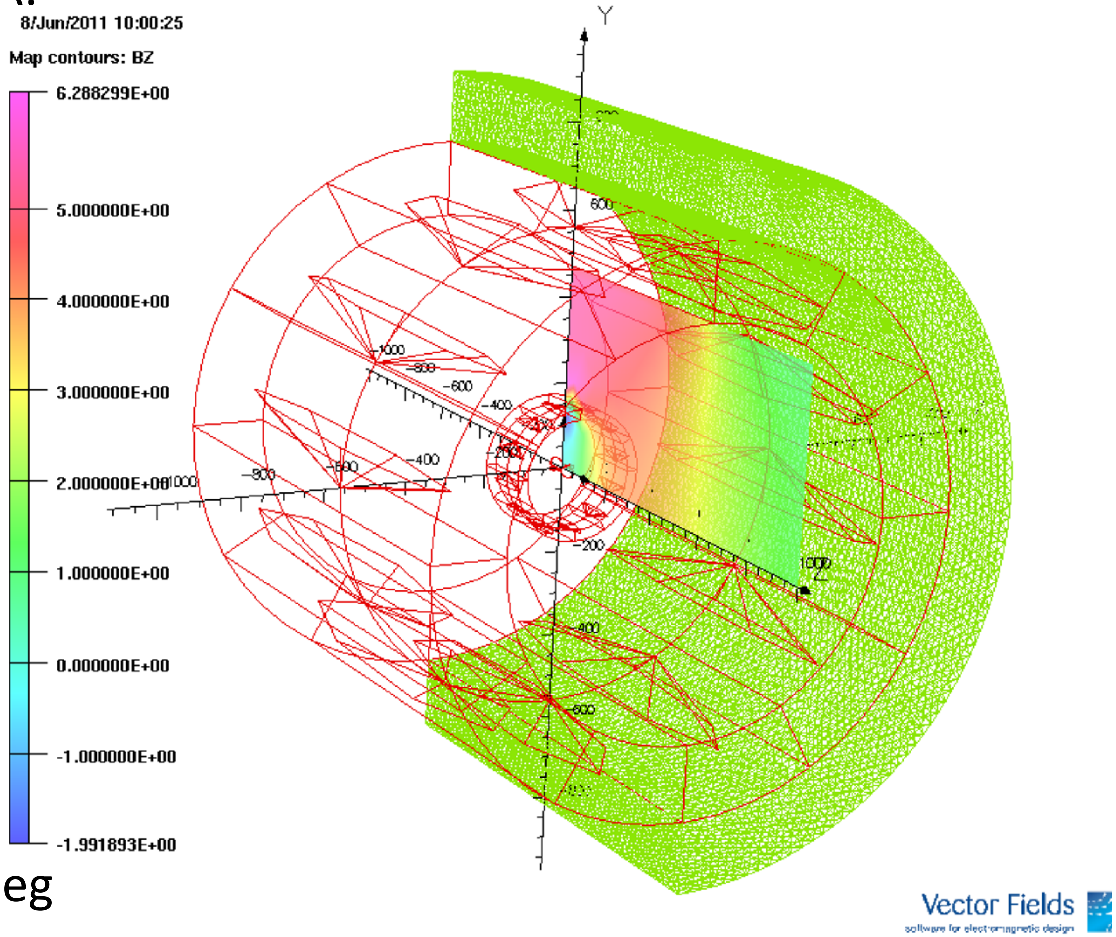

Evaluate different magnetic configurations

- field quality

target region, drift volume

- feasibility study

Constraints

- forward acceptance 30deg or 60 deg
- transverse acceptance 30 deg
- superconducting wires performace

Different superconducting wires and magnetic configurations loadlines are compared for a **realistic feasibility study**

Back up

Mean p/K separation (5-8 GeV/c)

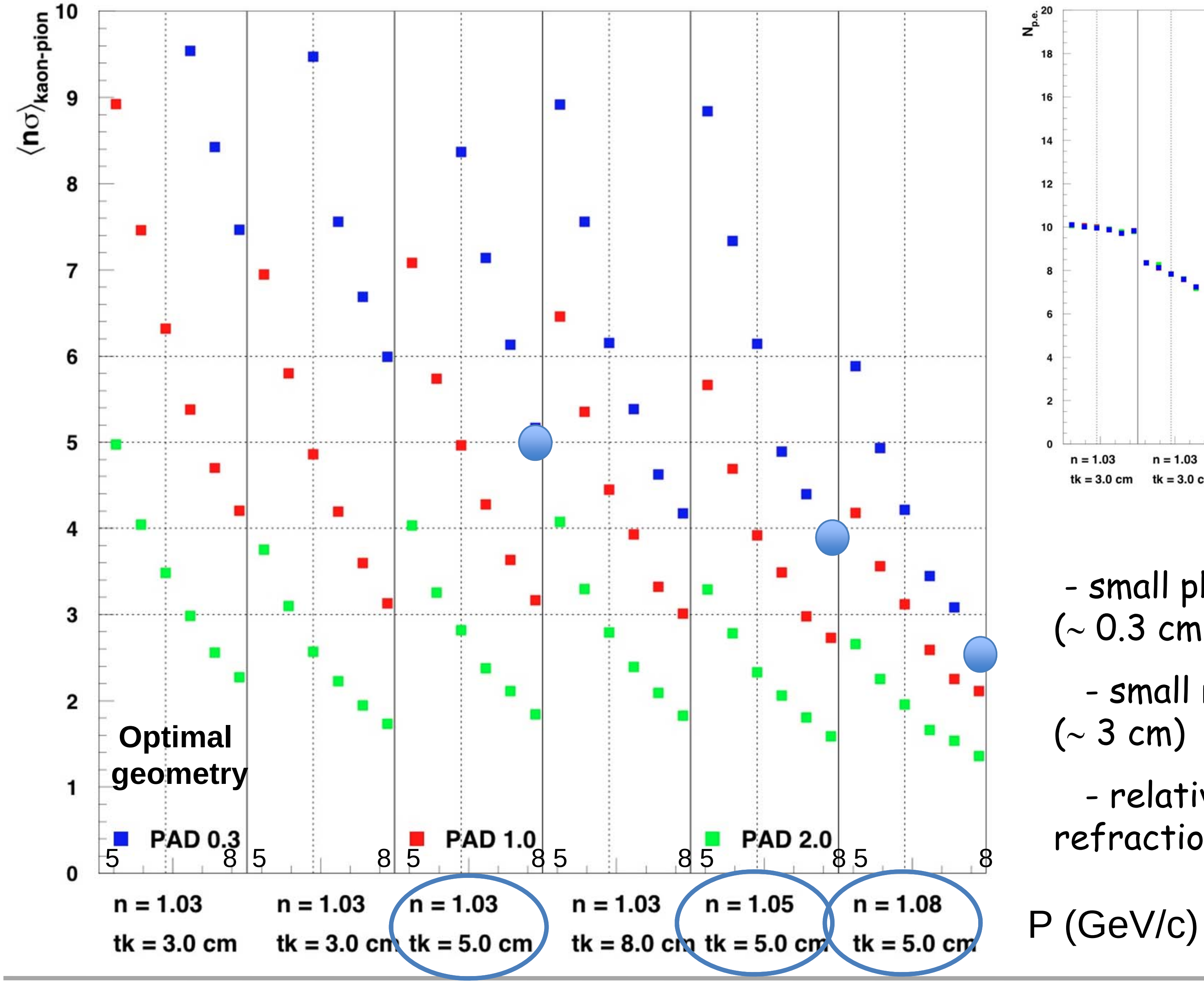

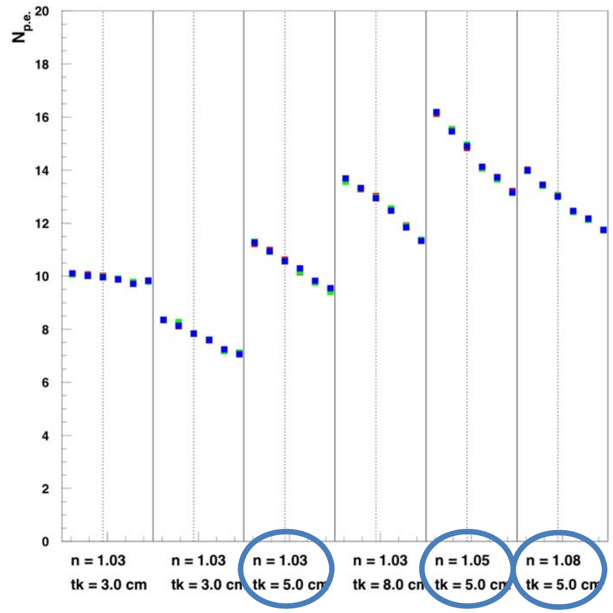

- small photo-detector pads (~ 0.3 cm)
- small radiator thickness (~ 3 cm)
- relatively small refraction index (~ 1.03)

Mean p/K separation (5-8 GeV/c)

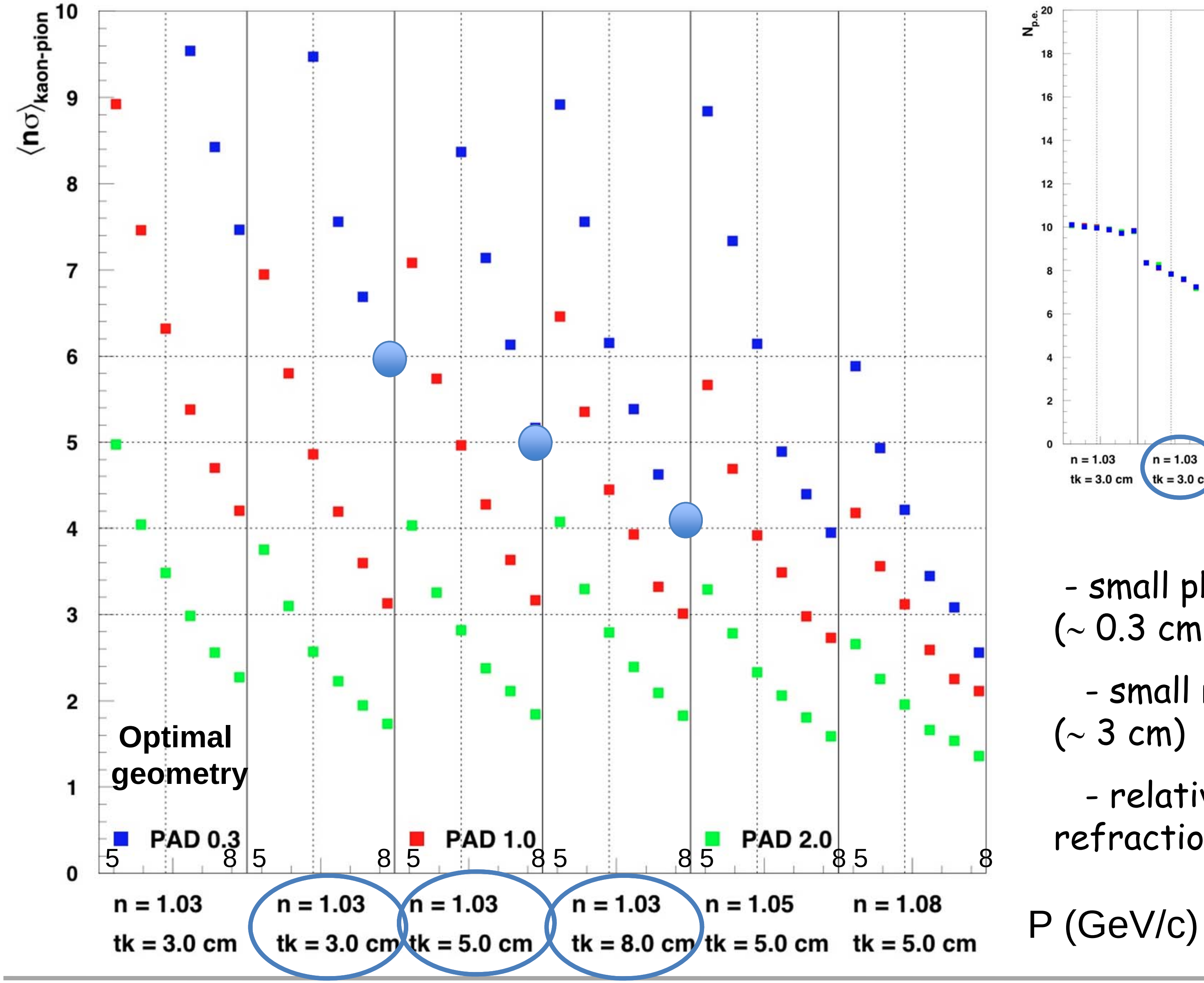

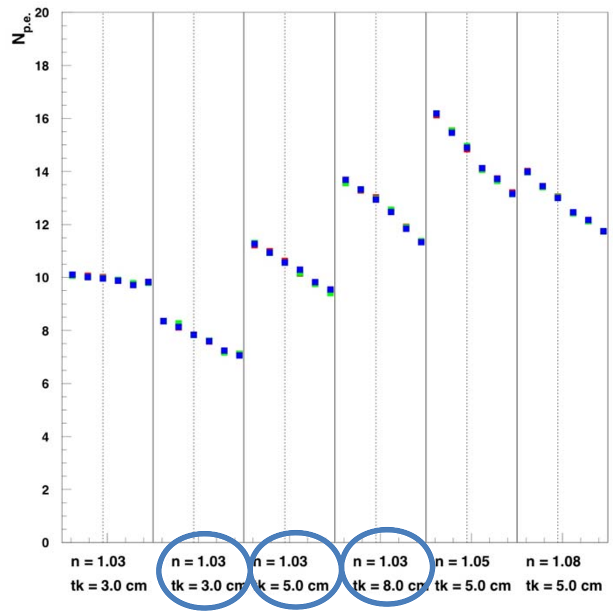

- small photo-detector pads (~ 0.3 cm)
- small radiator thickness (~ 3 cm)
- relatively small refraction index (~ 1.03)

Average N p.e. : PMTs: UBA

Mirror 14-25°

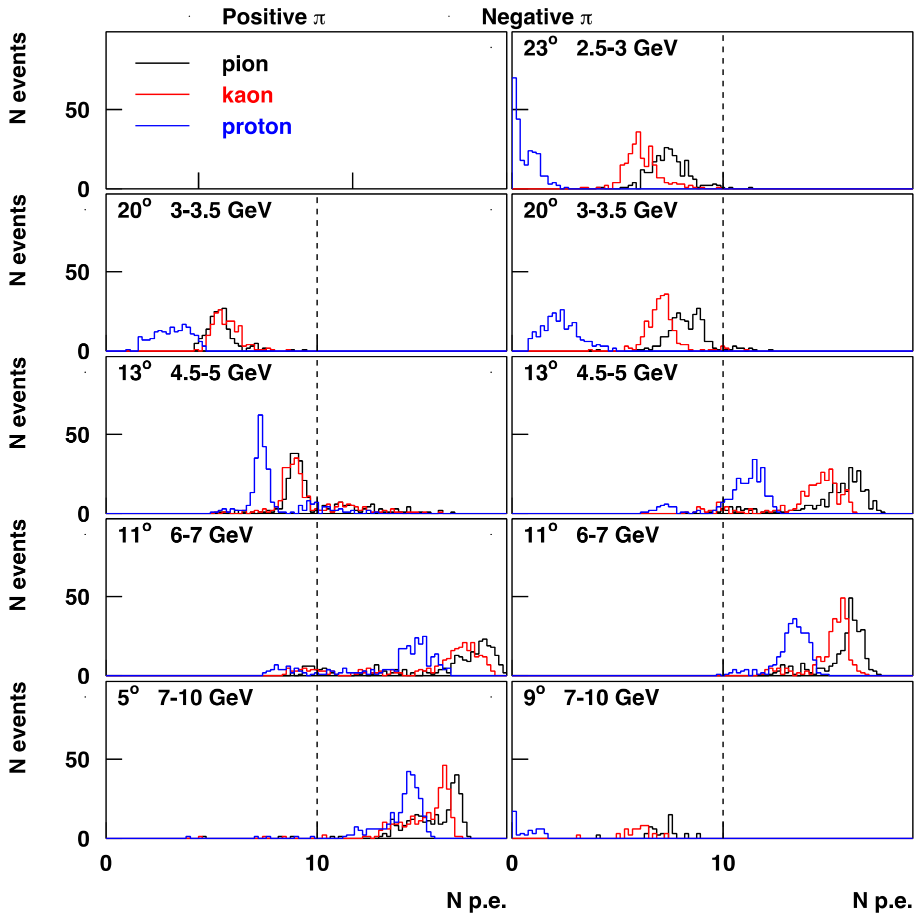

Mirror 14-35°

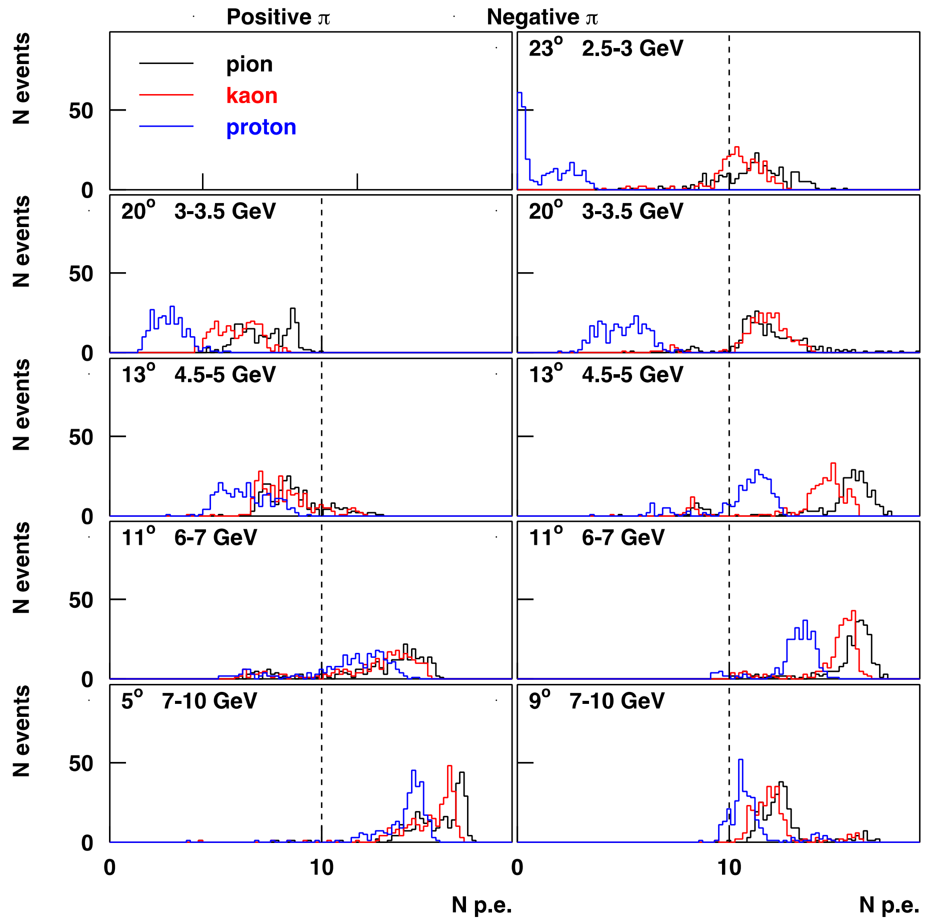

Worse for positive hadrons
Better for negative hadrons

LH_{π}-$LH_{k,p}$: PMTs: UBA

Mirror 14-25°

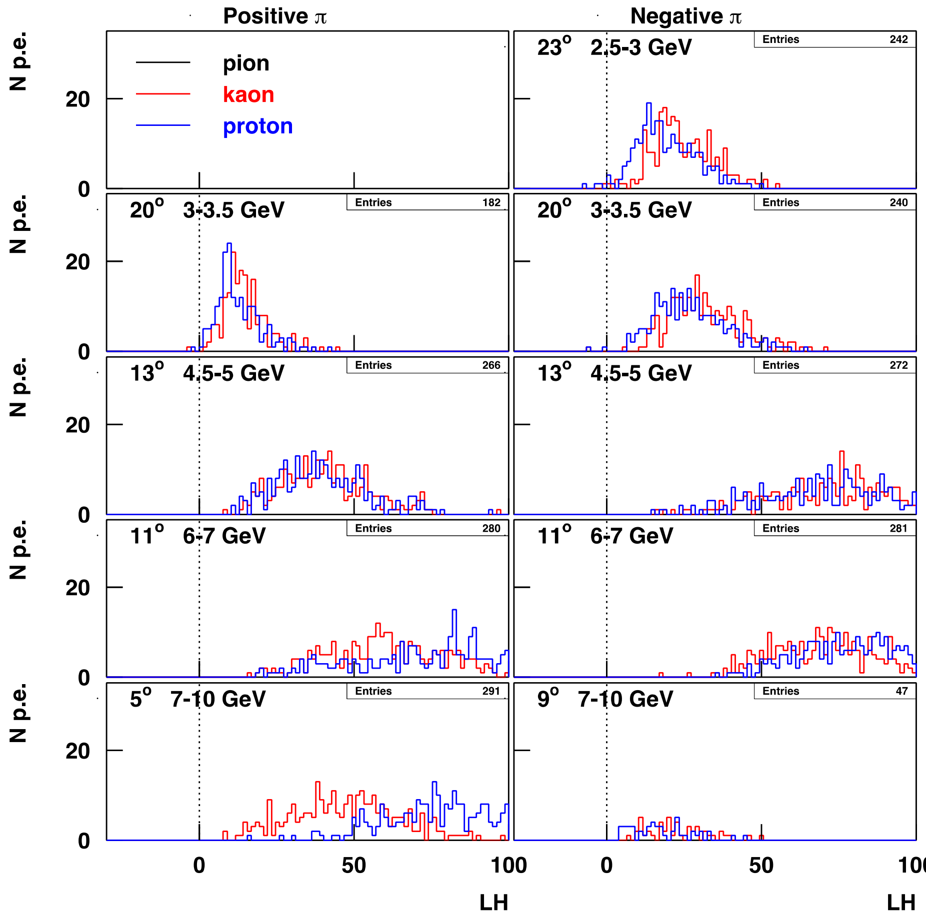

Mirror 14-35°

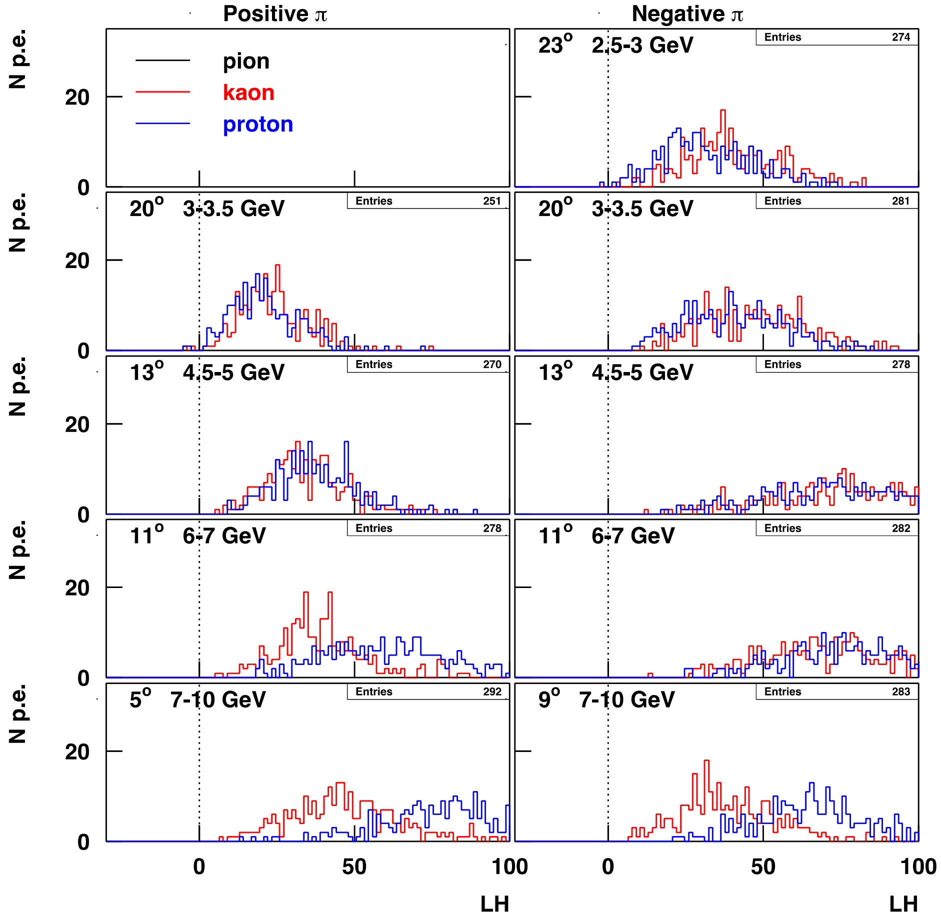

Worse for positive hadrons
Better for negative hadrons

Average N p.e. : Mirror Angle Coverage (UBA)

100 trials per point

Aerogel:
- n=1.06
- thick. increasing with radius: 2-4-6-8-10 cm

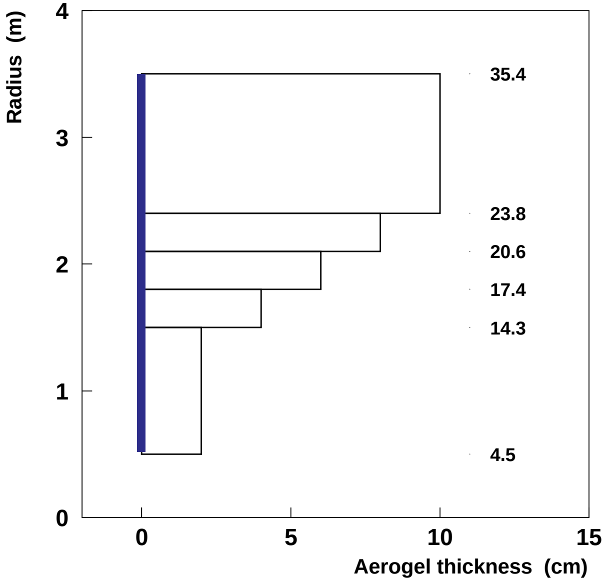

M35 is acceptanble but slightly worse for positive and does not improve at large angles ?!

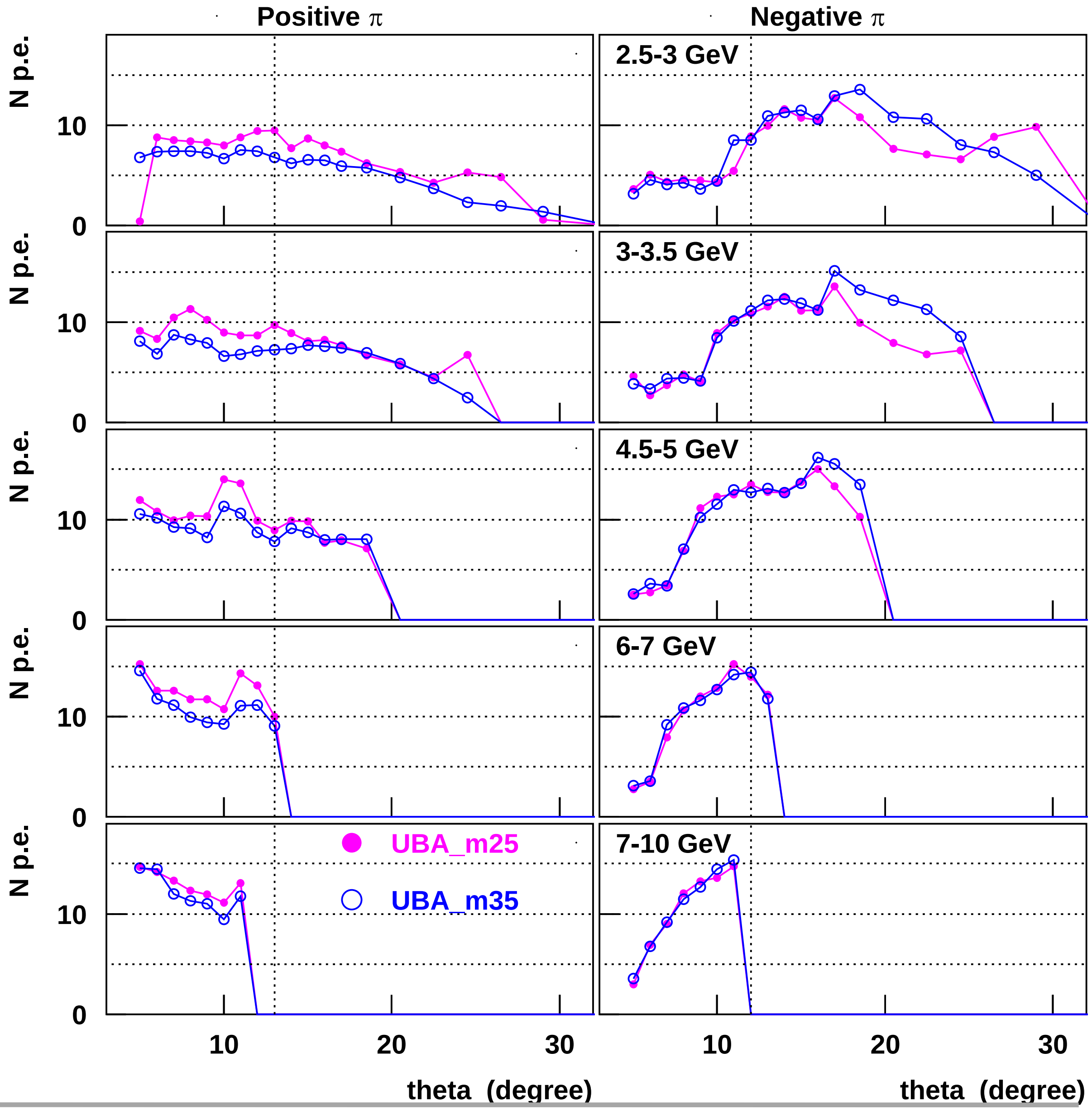

Average N p.e. : Mirror Semi-axes (UBA)

100 trials per point

Aerogel:

- n=1.06

- thick. increasing with radius: 2-4-6-8-10 cm

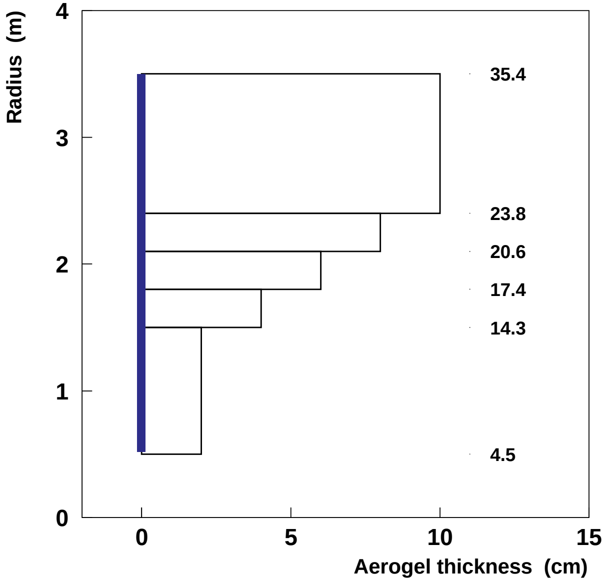

Symmetric Ellipsoide Semi-Axes focalizing onto the photon detector best in Npe

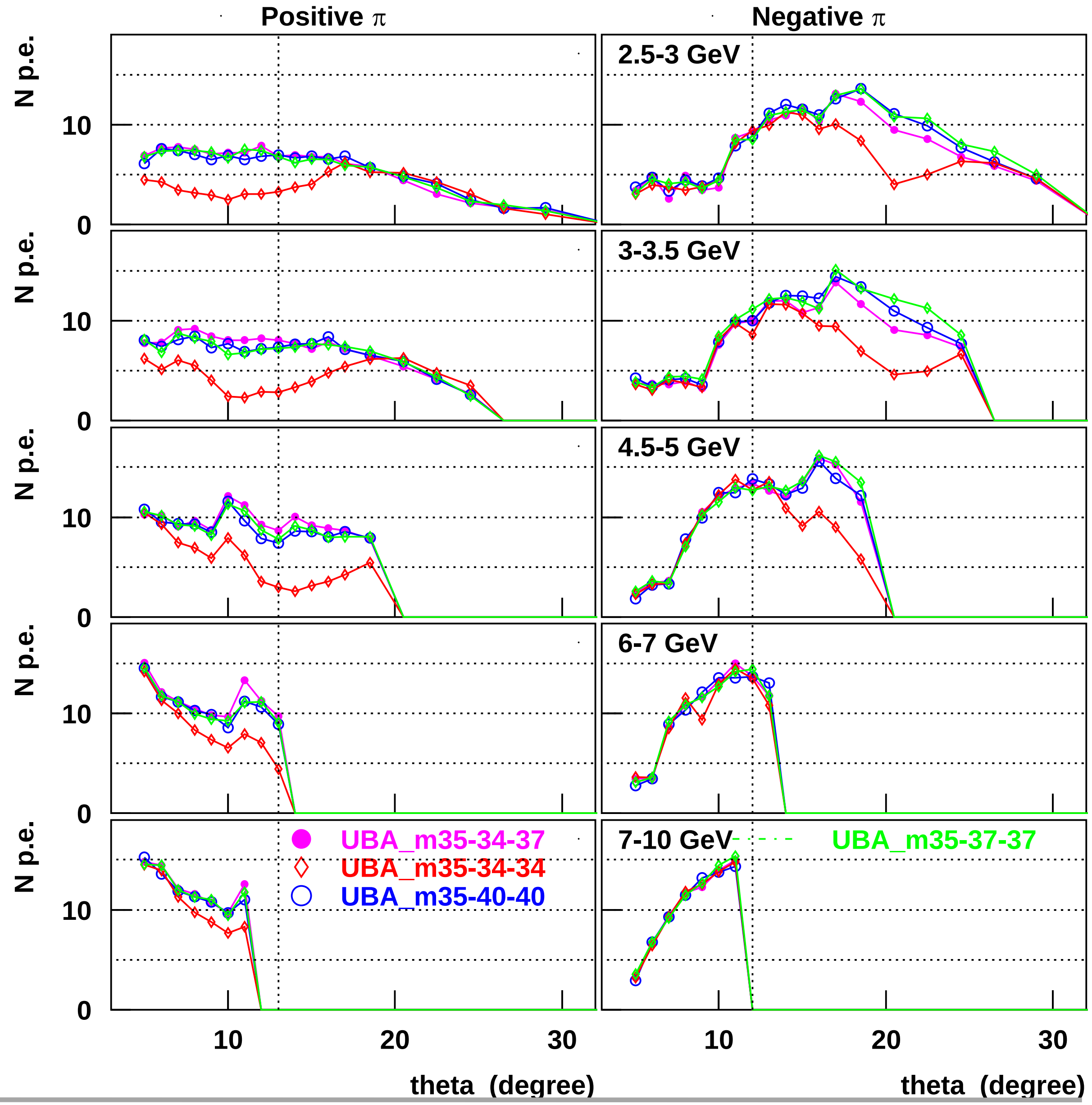

Feasibility study

Different superconducting wires and magnetic configurations loadlines are compared